

**In-Situ Vehicle Classification Using an ILD and a
Magnetoresistive Sensor Array
Final Report**

Prepared by:

Stanley G. Burns
Department of Electrical and Computer Engineering
University of Minnesota Duluth

January 2009

Published by:

Center for Transportation Studies
University of Minnesota
200 Transportation and Safety Building
511 Washington Ave. S.E.
Minneapolis, MN 55455]

This report represents the results of research conducted by the authors and does not necessarily represent the views or policies of the University of Minnesota and/or the Center for Transportation Studies. This report does not contain a standard or specified technique.

The authors, the University of Minnesota and the Center for Transportation Studies do not endorse products or manufacturers. Trade or manufacturers' names appear herein solely because they are considered essential to this report.

Acknowledgements

Funding was provided by the Northland Advanced Transportation Systems Research Laboratories (NATSRL), Center For Transportation Studies, University of Minnesota, and the University of Minnesota Duluth. (CTS/UMD). Banner Engineering provided the magnetoresistive sensor array and associated software.

Over the course of the project, electrical and computer engineering students Timothy Delf, Vikhram Gowreesunker, Jerod J. Wendt, James R. Riehl, and Zachery T. Serre as well as David J. Keranen (NATSRL staff engineer) assisted in the data collection and modeling. Their work was directed by Stanley G. Burns and is acknowledged in the individual chapters.

Table of Contents

Executive Summary:

Chapter 1: In-Situ Vehicle Classification Using an ILD and a Magneto-resistive Sensor Array

Appendix A: “Inductive Loop Detector Simulation and Analysis” by Vikram Gowreesunker and Zachary Gerbozy (undergraduate ECE students) is an initial software model design using the 3M donated Canoga Model Interface and data Acquisition Software (C8000IS). The model is based upon Wolfram Research MATHEMATICA™ 4.0. Report prepared May 8, 2002.

Appendix B: “ILD Simulation Users Guide” by James R. Riehl (Graduate student brought onto the project during the 2002 summer session) includes a MATLAB™ model along with comparisons to experimental data for several vehicle types. MATLAB™ became the preferred software package over MATHEMATICA™ because of cost availability and best utility to the data collection and modeling. Report prepared August 19, 2002.

Appendix C: “Inductive Loop Detector Simulation and Analysis” by Vikram Gowreesunker (undergraduate student but transferred to UMTC for graduate studies) is a summary of software and experimental results for the project through summer 2003. Report prepared August 26, 2003.

Appendix D: “An Overview of Using Magneto-resistive Sensor Arrays For Traffic Measurements” Prepared by Stanley G. Burns and Timothy Delf (graduate student in ECE).

Appendix E: Poster #2, “Inductive Loop Detector Vehicle Signature Analysis Using Magnetic Field models, Simulations, and Measurements” prepared by Stanley G. Burns, Timothy Delf (undergraduate ECE student), and Dave Keranen (staff engineer assigned to NATSRL).

Appendix F: Poster #1, “Inductive Loop Detector Signal Analysis”, prepared by Stanley G. Burns and Jerod Wendt (undergraduate ECE student). Poster outlines the custom software signal processing algorithms used to process ILD data with a dedicated differential inductance measuring system.

List of Figures

Figure 1	Magneto-resistive Array and ILD Sensor System
Figure 2	I-35 Test Site Marker 236 Southbound Aerial Photograph Provided by Mn/DOT
Figure 3	ILD Magnetic Field And Inductance Analysis
Figure 4	ILD Two-Dimensional Plot of Inductance
Figure 5	Cross-Section Inductance For An ILD And A Quadrapole

- Figure 6 ILD And Quadrapole Inductance As A Function Of Height Above The Road Surface. (Center Of The Loop)
- Figure 7 ILD Inductance Signature For An "18-Wheeler".
- Figure 8 Single Centered Magneto-resistive Orthogonal Axes Magnetic Field Deviations and Absolute Value (The vehicle under test was 3/4 ton Ford extended cab pickup truck with a snowplow mounting frame (without plow) and winch moving at 40 mph. One can easily observe the large ferrous-induced peak from the snowplow frame structure as well as the two smaller peaks from axles.)
- Figure 9 Seven Magneto-resistive Sensor Array Response For a 3/4 Ton Pickup With Snowplow Frame
- Figure 10 EXCELL Graphical Interpolation of the data In Figure 9
- Figure 11 Sample GUI Screen

Executive Summary

This document provides a summary of results from a multi-year study that includes both the use of inductive loop detectors (ILDs) and magnetoresistive sensors for in-situ vehicle classification. Several electrical and computer engineering students participated in the study and their contributions are included. Under my direction, these students also presented project work and Research Day conferences at MN/DOT District 1 Headquarters. Multiple Powerpoint™ presentations at various venues were not included.

This report does not include the following efforts although the interim quarterly reports do include this information.

- Design collaboration on the I-35 test site and infrastructure.
- Design collaboration, procurement and installation of ILDs, related sensors, and the associated wiring and interface to the Canoga systems and other instrumentation.
- Design collaboration, procurement and installation of the magnetoresistive sensor array and interface to the computer system.

In-situ vehicle occupancy, vehicle type classification, and speed are important measurements needed in traffic management. Most operational methods rely on threshold set inductance changes in the standard 6 foot square inductive loop detector augmented by limited use of video cameras and associated image processing. Typically, vehicle occupancy is determined by exceeding an eddy current induced inductance change threshold at a given ILD location. However, if one examines analytically and experimentally the time-dependent inductance change profile rather than the threshold switching level for establishing an occupancy number, there are unique signatures associated with different vehicle types. There appears to be correlation with vehicle structure both experimentally and in simulations; however, it is clear that the ILD large size, system sample rate, and the vehicle speeds precludes the differentiation needed for the numerous NHTSA classifications although major classes can be identified. Basically, the ILD cannot be treated as a spatial zero-width impulse sampled-data response system, which implies the spatial resolution is not adequate for vehicles moving at normal speeds.

Buried magnetoresistive sensors potentially offer another approach to obtain this traffic management data. The magnetoresistive sensor is a sensitive three-axis magnetometer with in-situ correction for the net vector magnitude 0.5 G Earth's magnetic field. The magnetometer responds to the local magnetic field perturbations resulting from the relative permeability change, μ_r , of ferrous vehicle subsystems passing over the sensor such as the frame and engine. The essentially point source nature of the magnetoresistive sensor with a 6 ms sampling time whose active sensing dimension is on the order of 2 cm results in 3 inch spatial resolution of a vehicle traveling at 30 mph. Consequently, one is able to differentiate between different portions of a vehicle such as the engine, frame, and axles by measuring magnetic field deviations. An array of these sensors can then be used to provide a unique in-situ mapping of a vehicle configuration.

Chapter 1

In-Situ Vehicle Classification Using an ILD and a Magneto-resistive Sensor Array APPROACH AND ANALYSIS

The basic approach was to model and measure a vehicle-induced time-domain inductance change, when using an Inductive Loop Detector (ILD) and the localized magnetic field perturbation when using a magneto-resistive sensor and compare the results analytically and experimentally. Figure 1 is a schematic diagram of both sensing systems located at a test facility, Figure 2, on a frontage road to the west of I-35, 20 miles south of Duluth, MN.

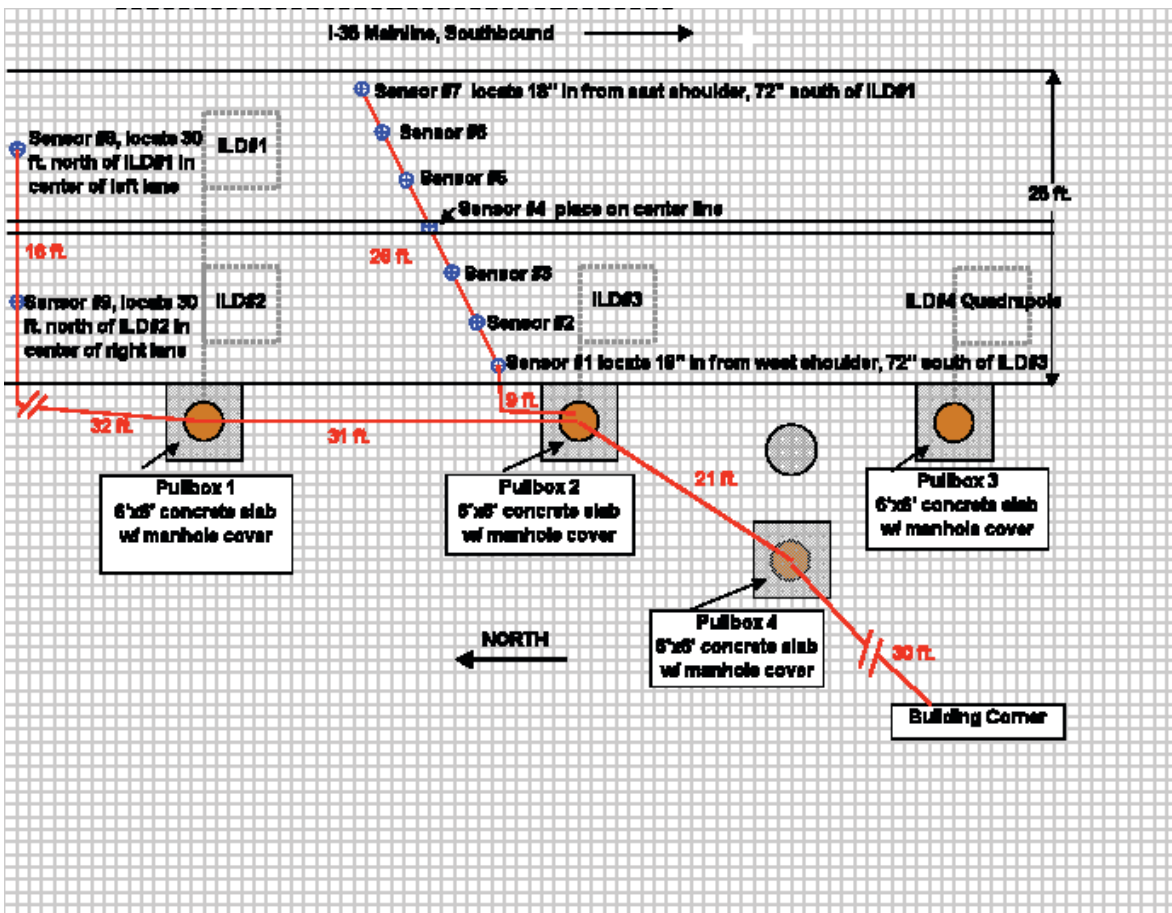


Figure 1 Magneto-resistive Array and ILD Sensor System

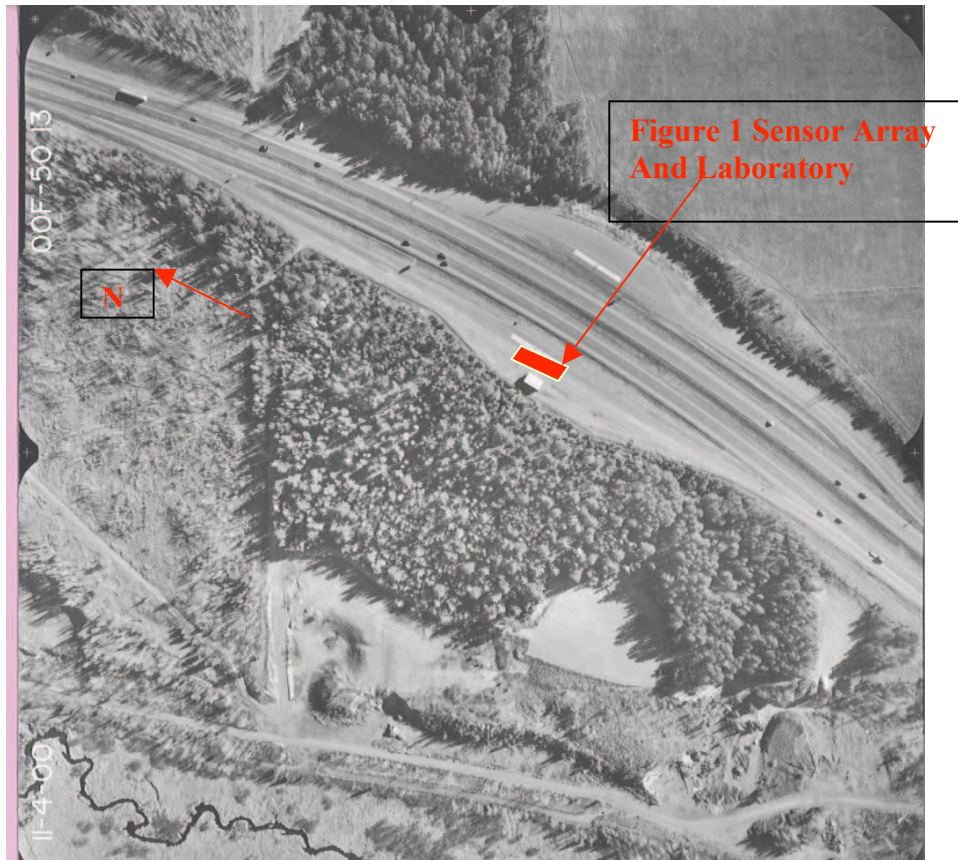


Figure 2 I-35 Test Site Marker 236 Southbound
Aerial Photograph Provided by Mn/DOT

The ILD, as a primary sensor system for traffic management has been use for decades.[1] The fundamental theory and equivalent circuits dates from the 1920's study of the behavior of flat pancake inductors used in early radio systems [2]. Much of the practical implementation and theoretical magnetostatics theory and background is summarized in Federal Highway Administration documents. [3]

Three standard 4-turn ILDs and one quadrapole are located as shown. An array of seven magneto-resistive sensors are positioned across both lanes of the frontage road. Two additional magneto-resistive sensors are positioned to serve as triggers. The spacing is designed for simultaneous collection of both ILD and magneto-resistive data including lateral and longitudinal inductance and magnetic field measurements.

ILD Time Domain Inductance Model

The measured inductance of an ILD decreases when a vehicle is within the active region of influence. [4]. This decrease in inductance is the result of induced currents, i.e. eddy currents, which significantly overcomes any net inductance increase from the increase in the relative permeability, m_r , of ferrous vehicle components such as the frame and engine. The resultant mutual inductance from the induced eddy currents requires a closed electrical path such as that provided by the vehicle frame, engine, and other, not necessarily ferrous, vehicle subsystems.

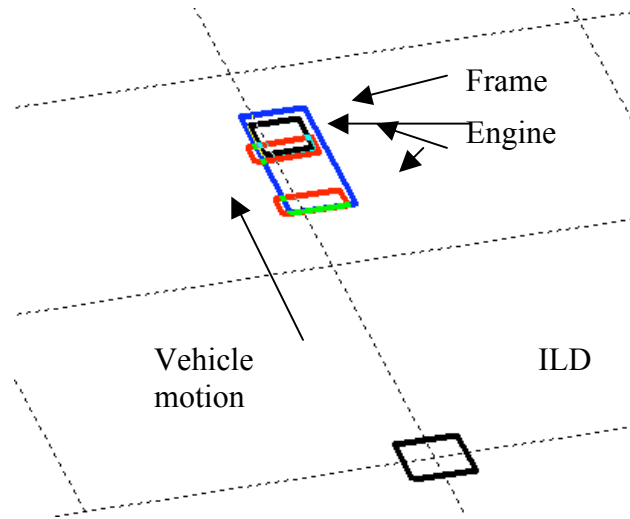


Figure 3 ILD Magnetic Field And Inductance Analysis

Figure 3 illustrates a four closed-path mutual inductance simulation model. The results of the simulation which will output a net negative inductance change of the ILD.

Assuming the ILD has negligible resistance and the length of one side of loop \gg radius of wire,

Biot-Savart's Law, as given below, is used to compute the magnetic field, B , and the magnetic flux density, Ψ , which is then used to obtain the ILD inductance, L , which then includes all of the mutual inductances M . Observe that there are mutual inductance interactions between all of the closed paths. Only four closed paths are used because of computational complexity. In reality, the vehicular structure is considerable more complex. MATLABTM was used for calculating the three dimensional ILD magnetic field and the resultant eddy current induced interaction with vehicles passing over the ILD. Eqn. (1) yields the ILD inductance.

$$L = \frac{N\Psi}{I} \quad (1)$$

and the flux density

$$\Psi_{21} = \int_{S_2} \mathbf{B}_1 \cdot \hat{n} dS \quad \text{also} \quad \Psi_{12} = \int_{S_1} \mathbf{B}_2 \cdot \hat{n} dS \quad (2)$$

must be computed for each closed path with the result for mutual inductance given by

$$M_{21} = \frac{N_2 \Psi_{21}}{I_1} \quad \text{and} \quad M_{12} = \frac{N_1 \Psi_{12}}{I_2} \quad (3)$$

Figure 4 illustrates the magnetic field intensity from a standard 1.83 m x 1.83 m ILD. The inductance is proportional the square of the number of loops in the ILD. The fringing magnetic field suggests that there may be adjacent lane phantom vehicle detection errors. Figure 5, illustrates this detection potential for both the standard ILD and to a lesser extent, for the quadrapole.

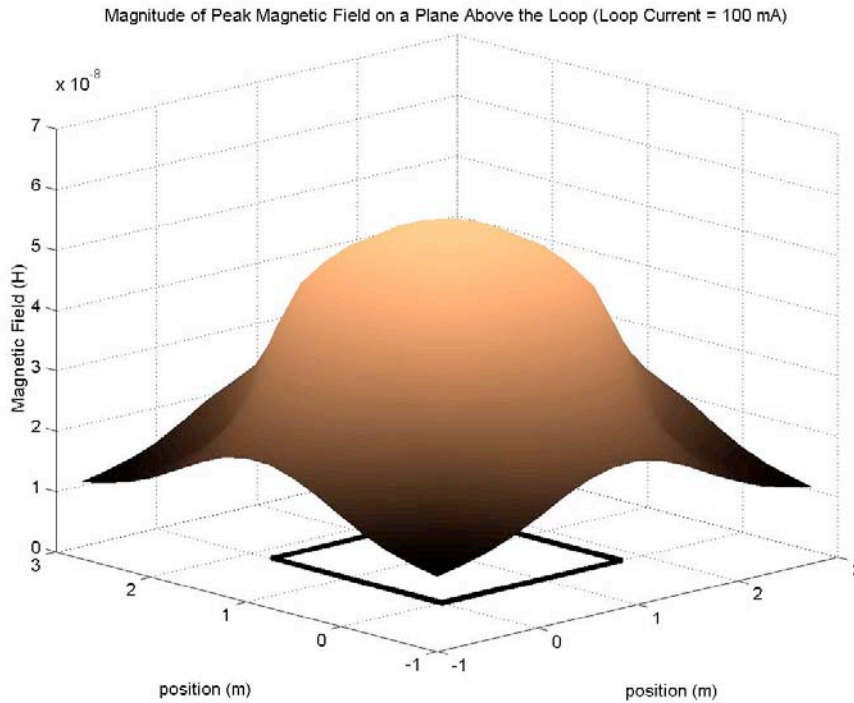


Figure 4 ILD Two-Dimensional Plot of Inductance

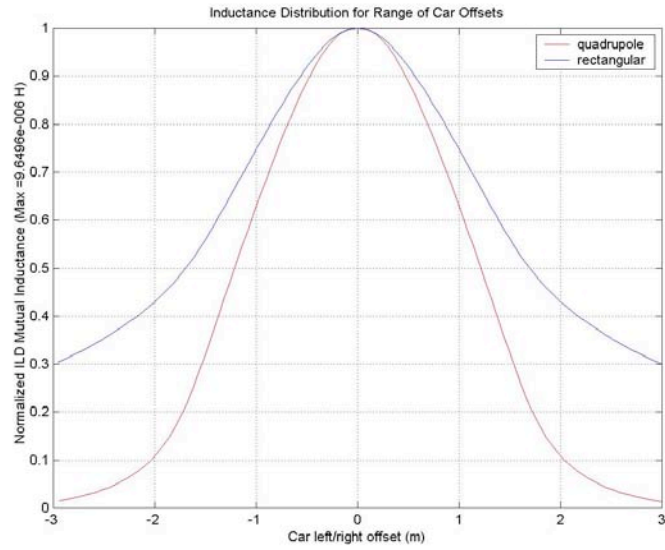


Figure 5 Cross-Section Inductance For An ILD And A Quadrapole

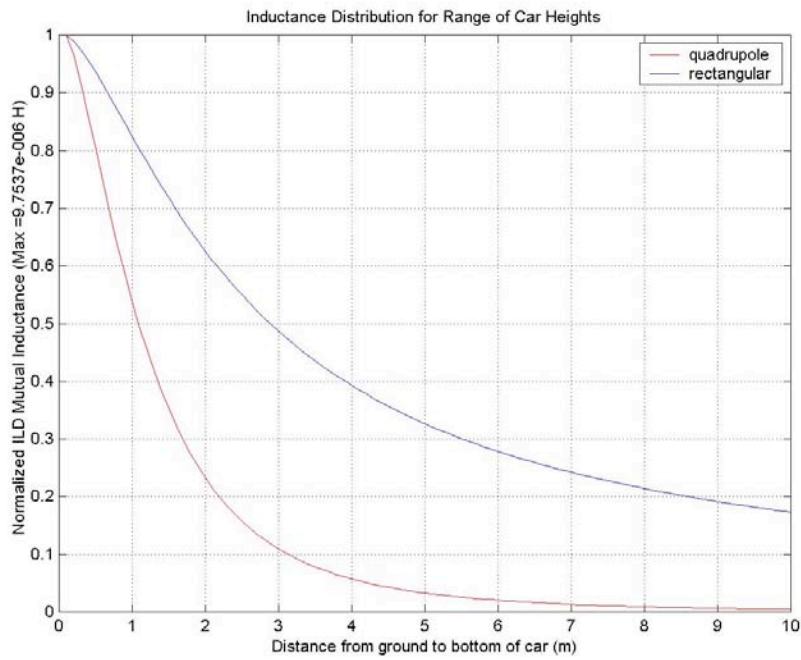


Figure 6 ILD And Quadrapole Inductance As A Function Of Height Above The Road Surface. (Center Of The Loop)

Figure 7 is an example of an ILD inductance signature obtained from a truck-trailer, “18 wheeler”. This time-domain signature is obtained by measuring the inductance every 30 ms using a LASER-triggered Agilent LCR Bridge. The inductance change from the engine/cab and axles are clearly visible. However to be more quantitative, several signal processing algorithms within MATLAB™ including first derivative signatures, n-order polynomial fits, and Fast Fourier Transforms (FFTs) have been employed to ascertain vehicle types. The measured signatures are also compared with two-four closed-path mutual inductance theoretical calculations using Eqns. 1-3. Closed path geometries were derived from an estimate of the vehicle frame, engine block, and axle dimensions. Preliminary studies on a limited number of vehicle types show that there are reasonably unique ranges of amplitude coefficients and response curves associated with different vehicles but the current 30 ms sample time measurement system does not provide adequate high vehicle speed resolution.

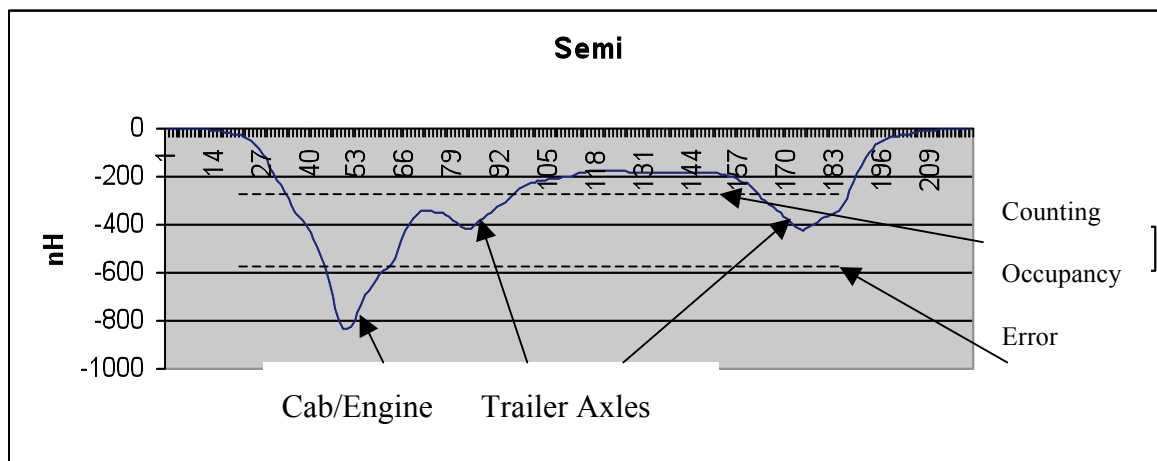


Figure 7 ILD Inductance Signature For An “18-Wheeler”.

Two different threshold settings are shown. The “Correct Count” threshold identifies occupancy for one vehicle of unknown type. The lower “Counting Occupancy Error” threshold indicates two vehicles. The velocity is under 10 mph. At higher speeds, the inductance profile becomes less defined.

Magneto-resistive Sensor Analysis

Magneto-resistance is the property of some materials to lose or gain electrical resistance under the influence of an external magnetic field. A modest 5% resistance reduction was first observed by William Thompson in 1857. Contemporary devices exploit the quantum mechanical effects observed in thin film structures fabricated from very thin alternating layers of ferromagnetic and non-magnetic materials. This Giant Magneto-resistive Effect (GMR) is exploited in computer magnetic hard drives. [5]

The magneto-resistive array being used for test site vehicle signature measurements is manufactured by Banner Engineering. Each of the seven sensors is an

active module which includes signal processing to reference the Earth's magnetic field and on-board non-volatile memory. [6] Each of the sensor packages includes three orthogonal magnetoresistive transducers and associated signal processing hardware. A serial data stream yields a 14-bit A/D digitized output voltage where a vector sum is computed using Eqn. 4.

$$V_{out} \propto (B_x - B_{ambient\ in\ x})\vec{a}_x + (B_y - B_{ambient\ in\ y})\vec{a}_y + (B_z - B_{ambient\ in\ z})\vec{a}_z \quad (4)$$

The magnitude of the Earth's magnetic field (vector sum of $B_{ambient}$ in x, y, and z at mid-latitudes is about 0.5 G) and is perturbed by nearby ferrous objects. Banner Engineering proprietary software is used to remove this quasi-static local magnetic field. Software is also used to remove temperature sensitivity. A key difference between the magnetoresistive sensor and the ILD is that the magnetoresistive sensor does not respond to non-ferrous metals, i.e. Al. Non-ferrous materials have a relative permeability of $\mu_r = 1$ while ferrous materials have $\mu_r \gg 1$ (usually 10s to several hundred). Consequently, the each of the magnetic field vector components is significantly and proportionally changed. This change, Eqn. 5, is what is measured and used to obtain signatures.

Figures 8, 9, and 10 illustrate the data available from the magnetoresistive array. All data is available in real-time. Figure 8 shows a single sensor magnetic field deviation from the background response in x, y, and z orthogonal axes as well as the net absolute value. The data intervals are 6 ms. The absolute counts in all seven sensors in the diagonal array to generate a signature as shown in Figure 9. When an EXCEL interpolation is applied, we have the solid profile shown in Figure 10.

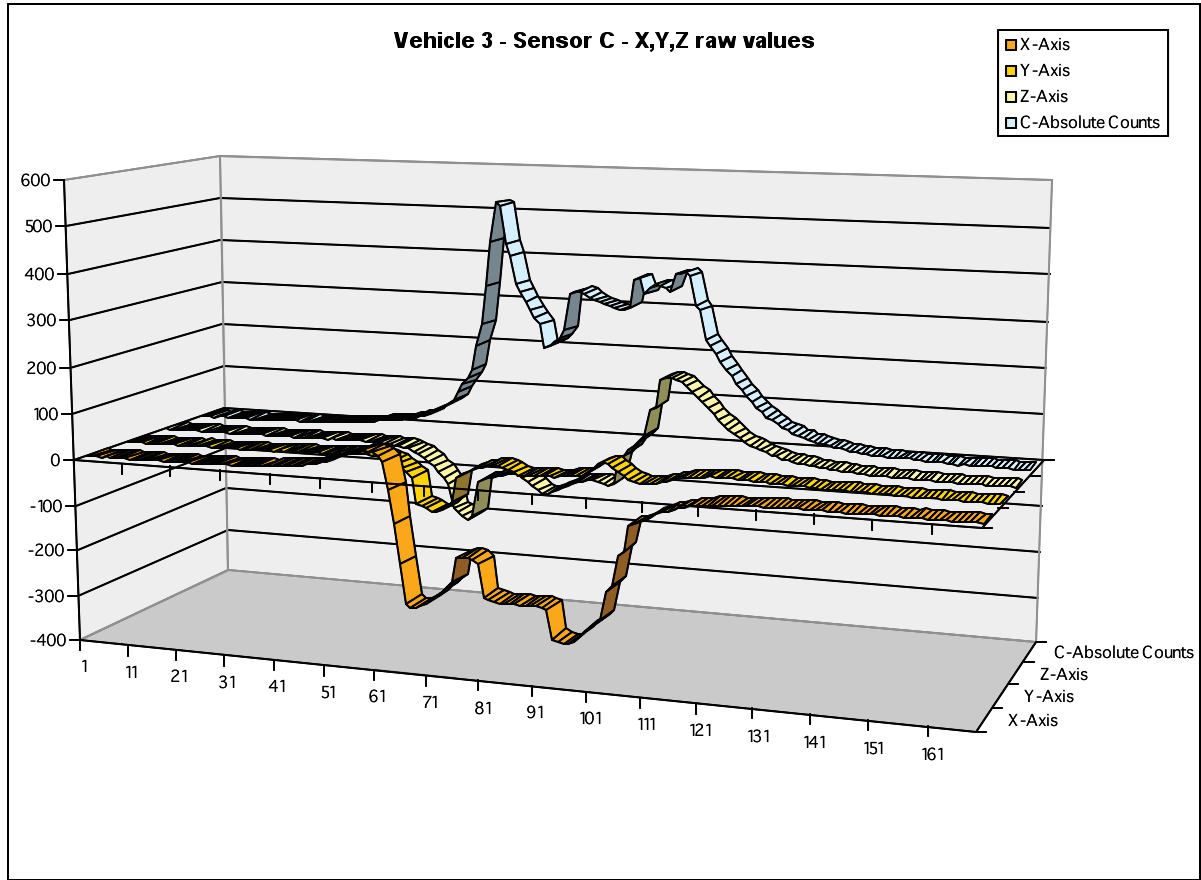


Figure 8 Single Centered MagnetoResistive Orthogonal Axes Magnetic Field Deviations and Absolute Value (The vehicle under test was 3/4 ton Ford extended cab pickup truck with a snowplow mounting frame (without plow) and winch moving at 40 mph. One can easily observe the large ferrous-induced peak from the snowplow frame structure as well as the two smaller peaks from axles.)

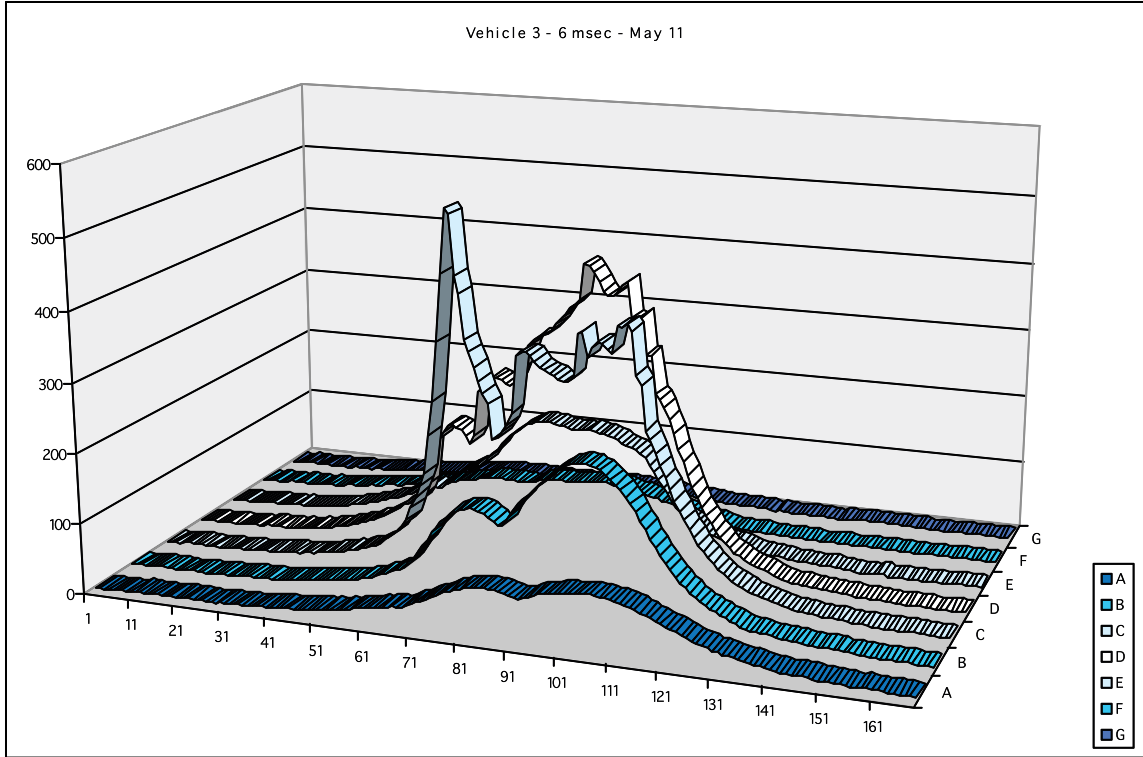


Figure 9 Seven Magnetoresistive Sensor Array Response For a ¾ Ton Pickup With Snowplow Frame

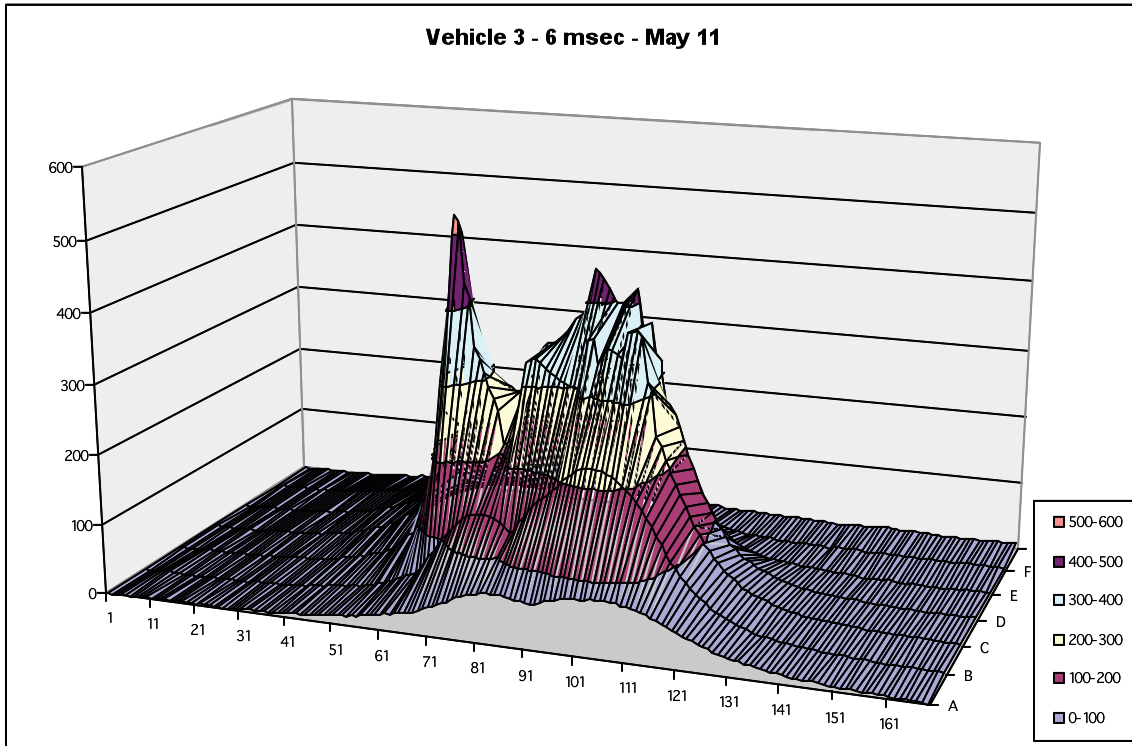


Figure 10 EXCELL Graphical Interpolation of the data In Figure 9

Summary and Directions Of Future Work

Both the ILD and magnetoresistive sensor systems have strengths and weaknesses when applied to vehicle classification and occupancy determination.

The ILD is, by far, the most widely installed sensor for traffic management. The ILD is a passive system which is generally reliable except for the stresses and strains that result in broken wires, etc. The threshold settings of the back-end electronics must be set such that smaller vehicles are not missed but if set too sensitive will falsely respond to adjacent lane vehicles and also to multi-axle vehicles. Results in reported in this report show that these threshold type errors can be minimized by various signal processing and recognition techniques applied to the measured, non-threshold, inductance profiles. However, the large sampling area of the ILD coupled with typical vehicle speeds reduces vehicular feature recognition accuracy. That is the primary reason single loop ILDs do not offer reasonable speed measurement accuracy. [7-9]

The magnetoresistive sensor is an active sensor which is also buried in the road surface but only requiring a single slit. Testing and deployment is limited. The long term reliability of an active buried sensor has not been established. There were several sensor failures attributed to packaging defects and these must be corrected and verified in a stringent testing program before additional experimental work is continued. There are issues with the software and error identification correction that also need to be addressed before the resumption of additional testing.

The magnetoresistive sensor is typically set up as a threshold sensor system for traffic management applications. However, results reported in this paper show that the effective “point source” impulse response provides far higher vehicle feature resolution at highway speeds. Signal processing and recognition software of the magnetic field perturbation signatures provide an opportunity for automated vehicle type identification if mechanical reliability and software issues can be successfully addressed. If two magnetoresistive sensors were located in the same diagonal slit at a know spacing and since the this inherently high resolution system could recognize the same vehicular structural feature, speed could be obtained directly. Backup video cameras, of course not usable at night, would not be required.

To facilitate data collection and analysis, MATLAB™ based GUIs (graphical user interfaces) have been developed for both the ILD and magnetoresistive sensor array as illustrated in Figure 11. This includes overlays for best fit polynomials that are used for the classification process.

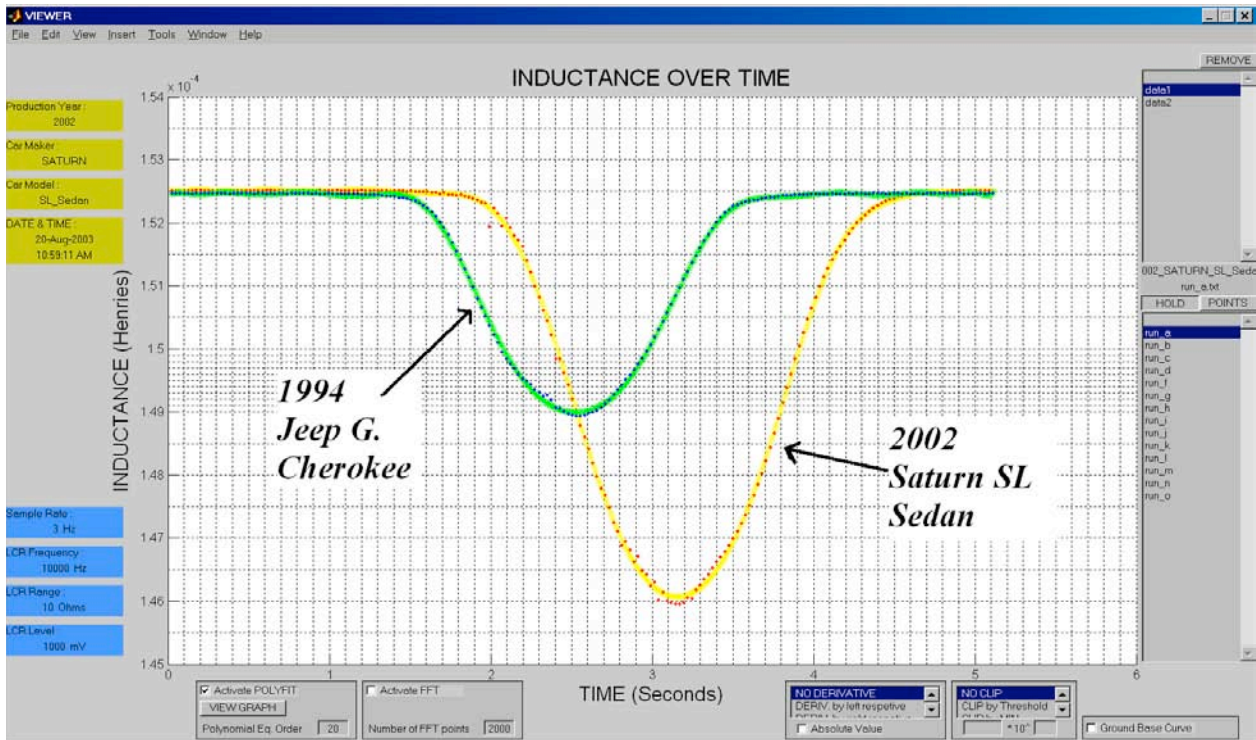


Figure 11 Sample GUI Screen

With a continuation of funding, future work will focus on:

- Preparing a three-dimensional model for different types of vehicles by mapping μ_r and use this model to predict the resultant local magnetic field distortion of a background ambient magnetic field. That is predict the resultant magnetic field distortion and resultant for a system of “chunks of iron” traveling across the sensor array.
- Comparing the model with field measurements of as many types of vehicles where classifications are delineated by the NHTSA.
- Working with the vendor(s) in reliability and software issue resolution.
- Comparing the magneto-resistive sensor signatures with the ILD signatures with respect to utility for vehicle classification, speed, and the specification of threshold setting criteria.
- Using the signatures for modeling and measurements of adjacent lane errors.

REFERENCES

1. *Inductive Loop Detectors*, ITS Decision Report, http://www.networking.eecs.berkeley.edu/...M/Incident_Manage/Detection/loopdet.html 1997 and 2001 updates. This site has extensive links to case studies, national and international, and assessments.
2. M. K. Mills, "Inductive Loop System Equivalent Circuit Model" *Vehicular Technology Conference of IEEE*, vol. 2, pp. 689-700, 1999.
3. *Traffic Detector Handbook, Second Edition*, Federal Highway Administration, Publication Number FHWA-IP-90-002, July 1990.
4. Carlos Sun, Intelligent Surveillance Using Inductive Vehicle Signatures, PATH, Rowan University, *Intellimotion*, Vol. 8, No. 3, 1999.
5. <http://www.research.ibm.com/research/gmr.html>
6. <http://www.baneng.com> Banner Engineering Corp. sensor technical data and http://www.bannerengineering.com/whats_new/release.php?id=71
7. Benjamin Coifman and Zu-Hsu Lee, *Estimating Median Velocity Instead of Mean Velocity at Single Loop Detectors*, Transportation Research-B, 7/11/2000.
8. Benjamin Coifman and Zu-Hsu Lee, *New Aggregation Strategies to Improve Velocity Estimation From Single Loop Detectors*, California PATH Working Paper, UCB-ITS-PWP-2000-12. August 2000.
9. Carlos Sun and Stephen G. Ritchie, *Individual Vehicle Speed Estimation Using Single Loop Inductive Waveforms*, California PATH Working Paper, UCB-ITS-PWP-99-14. October 1999.

Appendix A

Inductive Loop Detector Simulation and Analysis

Prepared by

Vikram Gowreesunker and Zachary Gerbozy

Under the Supervision of

Stanley G. Burns

May 8, 2002

Overview

Inductive loop detectors are used extensively in traffic control systems because of their high accuracy and non-intrusive characteristics. As a car passes over the loop its ferromagnetic undercarriage causes eddy currents to lower the inductance of the loop. The current application of the detector is to set a threshold for the change of inductance and thereby sense the presence of a vehicle. The purpose of this research project is to create a simulation of the continuous inductance change over time. This simulation was then compared with data collected from recently installed loop detectors at the NATSRL research facility. The resulting inductance information may lead to further identification of the vehicle being detected and single loop speed.

Inductive loop detectors (ILDs) are a proven and effective method of vehicular detection in modern transportation systems. The data obtained from these devices has been found to be extremely accurate, highly reliable, and low-maintenance compared to other similar technologies. It is for this reason that the ILD is the most widely used detection method in modern traffic control systems. Currently, the data extracted from a detector is the digital presence of a vehicle over the loop. The analog representation of the inductance change gives a better picture of the type and speed of the vehicle detected. If it is possible to collect this information through already installed ILDs, it could be obtained at a significant cost savings compared to another technology. Therefore, the purpose of our research is to simulate and verify the loop inductance as it changes during vehicle detection.

The inductive loop detector consists of a solenoid loop of wire buried underneath the pavement with the symmetric axis perpendicular to the road. The loop is connected via lead wire to an external circuit that measures its inductance according to a specific resonant frequency. The loop is supplied with a low current source, which creates a magnetic field and self-inductance of the loop. When a vehicle with an undercarriage of mostly ferromagnetic material passes over the loop, two factors cause the loops inductance to change. First, the magnetic permeability of the vehicle will raise the inductance of the loop due to the increase in flux density. Eddy currents induced by the vehicle that generally causes a decrease in the flux density overcome this change. The result is that the inductance of the loop is lowered and the detector counts the vehicle if that inductance change is greater than a certain threshold.

The basis for the computer simulation is to model the specific loops located at the NATSRL research facility. There are a total of four loops, three square loops and one quadrapole, made up of #12 AWG wire buried approximately two inches below the pavement. The loops are connected via pull boxes, which lead into the research facility and connect to the 3M Canoga C824T loop detector. The inductance of the loop is measured and processed by the detector before being sent to the computer.

Equipment

The computer simulation was performed using the Mathematica 4.0 program. This software allowed the simulation to have an adequate balance between its high computational and graphical demands. Testing of the simulation required the installation of a 3M Canoga vehicle detection system. The research team connected and successfully configured the following equipment to obtain data from the loops:

SOFTWARE

- ✓ Wolfram Research Mathematica 4.0
- ✓ 3M Canoga Model C800 Interface and Data Acquisition Software (C800IS)
- ✓ Camtasia 3.0.1 screen capture program
- ✓ Microsoft Excel 2002

HARDWARE

- ✓ 1, 6' X 6' Square Loop (4 turns of #12 AWG wire)
- ✓ 1, 3M Canoga Vehicle Detector (C824T)
- ✓ 1, 3M Canoga Power Supply Unit (R124A)
- ✓ 1, RTC Detector Card Rack (CR54W)
- ✓ 1, 4' X 4' plywood mounting board
- ✓ 1, Gateway desktop computer
- ✓ 1, RS232 serial port cable

The power supply required a separate unit to safely connect the necessary 120 VAC to the card rack, which disperses 24 VDC to each of the four vehicle detector slots. The power supply and card rack are mounted to a plywood board for convenience.

Methods

The magnetic field of a 1-turn 6x6 ft loop detector was simulated using Mathematica™. The first step in this simulation was to derive the three dimensional equation of the magnetic field for the loop. As shown in Figure 1, loop is defined to be located on the $Z = 0$ plane in the first quadrant of the Cartesian coordinate system.

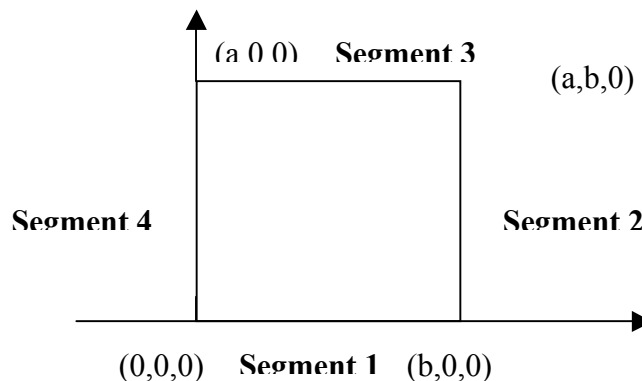


Figure 1. Diagram of Square Inductive Loop for Simulation

The loop is divided into 4 segments, and the magnetic field intensity at a point in space from each isolated segment was computed using the Biot-Savart law. Therefore, the magnetic field B is given by,

$$B = \mu * H$$

where

μ is the permeability of the material (H/m)

and

H is the magnetic field intensity (ampere-turns/m).

Using superposition, the corresponding vectors were added and displayed as a plot of the magnetic field surrounding the loop.

The inductance simulation required the selection of a method of calculation as well as selection of the proper equations to achieve an accurate model. The three primary methods of inductance calculations considered were LINK coupling, mutual coupling, and NIWA current sheet of which the mutual coupling method was the most appropriate. An outline of the mutual coupling method is given below.

- a) Computing external inductance of a wire segment [2]
- b) Generate equation to calculate Real and Imaginary Bessel functions and their derivatives. [1]
- c) Computing internal inductance of a wire segment using (b). [2]
- d) Compute total inductance of wire. [2]
- e) Computing the equation for Mutual Inductance between 2 parallel filamentary wires. [2]
- f) Use (c) to calculate the Mutual Inductance between 2 parallel rectangular loop. [3]
- g) Use (d) to compute the Mutual Inductance among the 4 parallel loops. [3]

A similar simulation for the self-inductance was also shown using a more basic method that does not incorporate the Bessel functions. A comparison between the two methods shows that there is a constant difference in the self-inductance where the more advanced simulation is more accurate. The more important information, the change of inductance (ΔL), remains consistent through both simulations.

When a car passes over an ILD, an eddy current forms by virtue of Faraday's Law and a resulting self-inductance develops in the car. The eddy current's magnetic field will oppose that of the loop (Lenz's law) causing a drop in the loop's inductance. There are no specific formulas for the complex geometries of vehicles therefore we must use an approximation. The two main geometries that were considered were a current loop and a current sheet, each with dimensions similar to those of the undercarriage of the car. The sheet method prevailed because it was the easiest to model under the restrictions imposed by movement. The sheet formula used to calculate the inductance of a vehicle.

$$L_{car} = (\mu * \mu_0 * h * x) / w.$$

Using this calculation,

μ is the permeability of the pavement (in H/m),

t is the thickness of sheet (in meters),

b is the width of the car (in meters),
 and x is the length of the vehicle covering the loop (in meters).
 With the sheet method, the effective inductance of the vehicle changes as more or less of the vehicle covers the loop. This simplification is not possible with the loop method and therefore it was not practical to use.

The final aspect of the inductance calculation is the mutual inductance equation. The basic equation for mutual inductance between two circuits is,

$$M_{12} = k * (L_1 * L_{car})^{1/2},$$

where k is the coupling coefficient. The resulting total inductance of the loop is then calculated by the formula,

$$L_T = L_1 - M_{12}.$$

y m

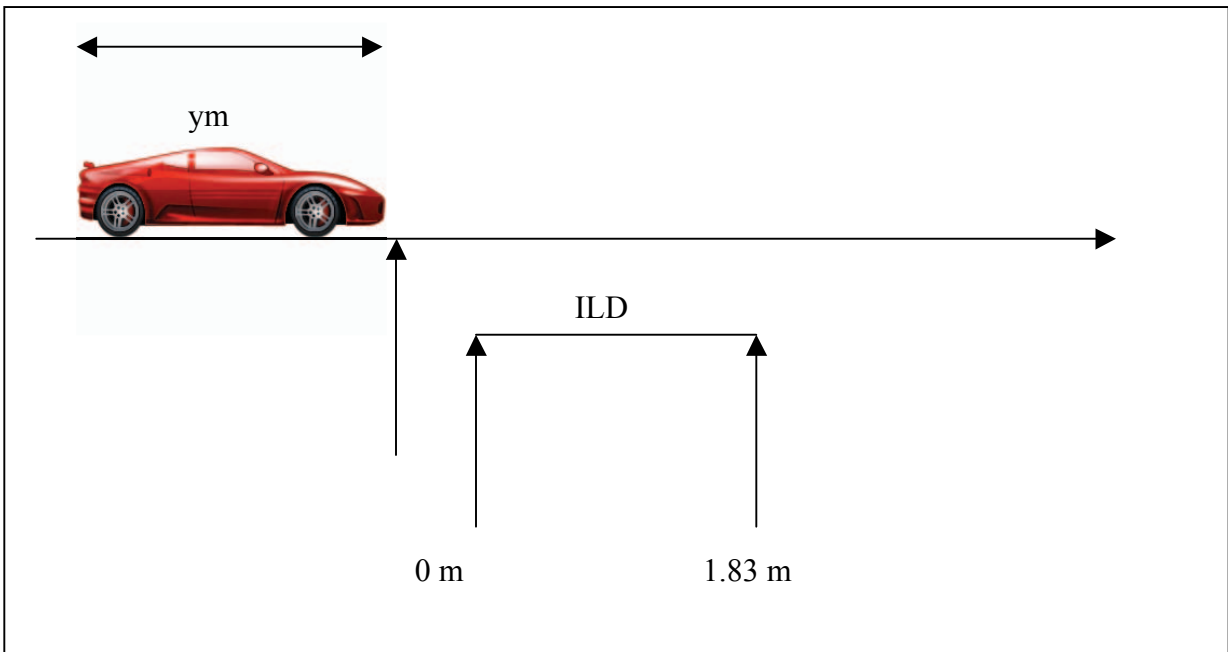


Figure 2. Diagram of Vehicle Position for Inductance Simulation

Since the equation for the inductance of the vehicle (L_{car}) is only non-zero when some of the vehicle is over the loop, the mutual inductance is only valid under this condition. Figure 2 shows the relative positions of the loop detector and vehicle for the simulation.

The measurements of the inductance were taken manually from the NATSRL research facility. The 3M Canoga data acquisition software does not include a program to record or detect the inductance versus time. The software only allows measurement of the total change of inductance. Therefore, to collect inductance versus time data the research team

positioned a car over varying amounts of the loop and backed away from the loop to measure the inductance change. Measurements were taken and repeated at least four times for various distances between 0 and 1.83 meters (the length of the loop). The measured change in inductance was then considered to be the inductance of vehicle at that position. A graph of the measured data was created and fitted with a 3rd order polynomial to show the estimated continuous function of inductance versus distance.

The final step to completing our verification is to relate the measured data for inductance versus distance to the inductance versus time function. The velocity of the vehicle as it passes over the relatively small distance of the loop should remain constant. Therefore by definition of the velocity, the distance should be equal to the velocity multiplied by the time,

$$\text{Distance} = \text{Velocity} * \text{Time}.$$

Thus, the two graphs will be equal when the velocity is 1 meter per second. This is equal to a speed of approximately 2.23 miles per hour, which is slow for most applications. Therefore, there will generally be a difference in scaling between the time and distance functions, which will depend on the speed of the vehicles being detected. This means that the measurements taken with respect to distance should show a wider and more accurate depiction of the inductance as it changes.

Results

The simulation of the magnetic field resulted in an enhanced visualization of the magnetic field. Figure 3 shows the vector plot simulation of a six-foot square loop similar to the ones used at the NATSRL research facility.

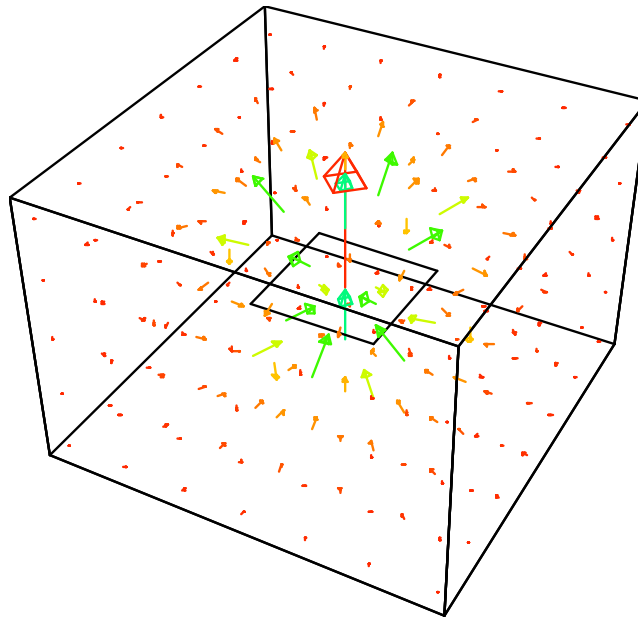


Figure 3. Magnetic Field Simulation of a Square Loop

The magnetic field lines follow the right hand rule corresponding to a counter-clockwise current flowing through the loop. The difference in colors and length show the intensity of the field lines having the greatest magnitude in the center and decaying rapidly away from the loop. A measurement of the actual magnetic field was not acquired due to lack of equipment.

The loop self-inductance simulation and measurement show slight variation in numerical results. The self-inductance calculations from the basic simulation are 158 μH and 142 μH , while the more advance simulation gives an inductance of 124 μH . The basic simulation results do not depend on the frequency of the current supplied to the loop or the radius of the wire.

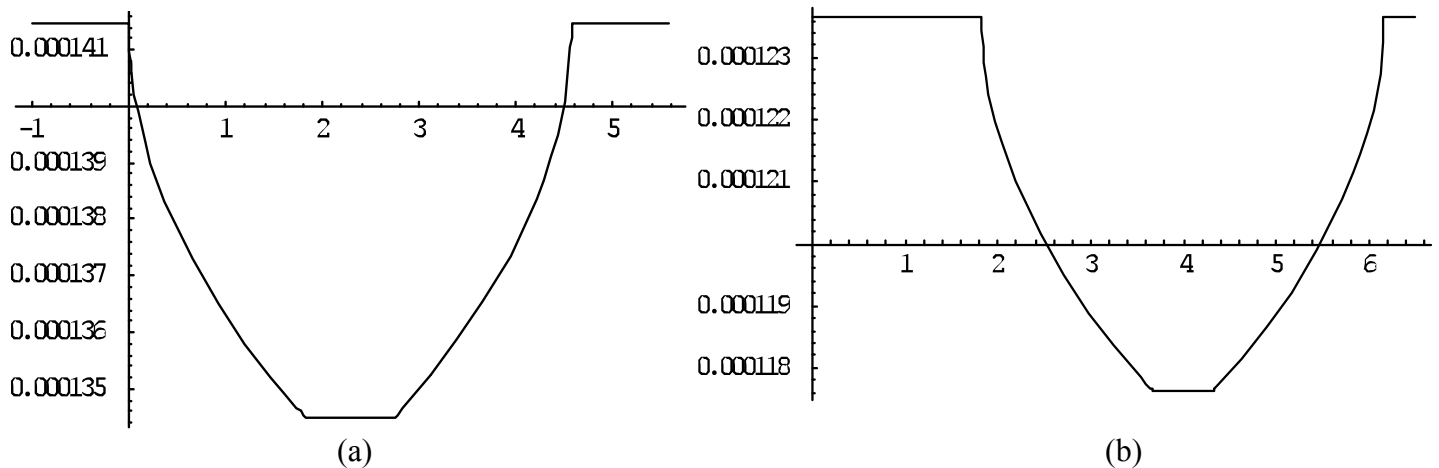


Figure 4. (a) Basic Inductance Simulation (b) Advanced Inductance Simulation

The measured self-inductance was approximately 124 μH , however, increasing the current frequency supplied to the wire causes the self-inductance to drop.

The constant differences in self-inductance simulations do not effect the change of inductance as a vehicle is detected. The inductance change (ΔL) was calculated for both cars to be approximately 6000 to 6500 nH. The measured inductance changes as shown in Figure 4 are approximately 6000 nH. One of the similarities between the simulation and testing data are the appearance of a plateau where the car fully covers the loop. This similarity is also shown in the measured inductance data.

One of the major disadvantages of the simulations is the abrupt change of inductance as the vehicle begins to cover the loop. Figure 5 shows the measured inductance with a 3rd order polynomial fit. The graph shows that the inductance change occurs more smoothly than the simulation.

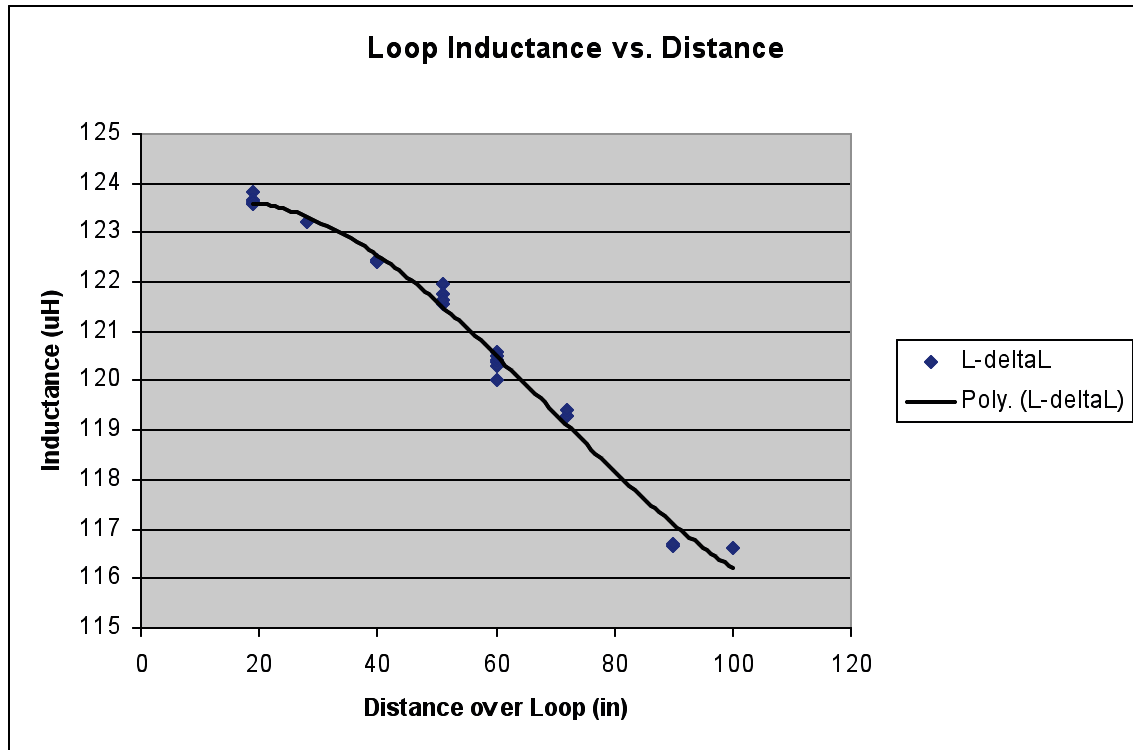


Figure 5. Inductance vs. Distance with 3rd Order Polynomial Approximation

The measured data from Figure 5 does show that the recorded change of inductance is approximately equal to the simulation change of inductance (from Figure 4). The disadvantages of this manual calculation of the inductance versus distance are the amount of time spent collecting data and the increased possibility of error. It took approximately four hours to collect one half of the inductance versus distance graph. The measurements had to be repeating many times because it was not possible to have the vehicle stop exactly at the measured point. The next step for this research is to find a way to more quickly and accurately measure this inductance versus time/distance data.

Discussion

The results of our research show the inductance vs. distance (time) plot for a vehicle and the supporting simulation of this event. This plot can be thought of as a signature for a particular type of vehicle traveling at a particular speed. This information could lead to more advanced vehicular identification utilizing the existing technology. In order to successfully develop these models, however, research would need to be conducted to develop these signatures more quickly, accurately, and easily.

Data acquisition research for the inductive loop detectors could be approached from either an analog or a digital perspective. The analog approach to obtaining the signatures would involve the purchase of a frequency to voltage converter applied to the outputs of the inductive loop. The signatures could be then recorded using a Modulation Domain Analyzer, Labview software and a GPIB board. This method could require a detailed schematic of the circuitry of the loop detector. Another approach would be to analyze the digital information sent by one of the Canoga C800IS software programs, which displays the real-time inductance data. A Visual Basic program could capture and show this data, however, a more detailed understanding of the software program is required for this approach.

Following a data acquisition project, a research team could extensively test different vehicles to obtain signatures for analysis. These signatures could be used compared with a fuzzy logic rule base to deliver the vehicle type information. Speed detection from a single loop is also possible through advanced signal processing algorithms for determining the vehicle length.

Conclusions

The research shows the possibility to obtain more information from an inductive loop detector. The inductance versus time (or distance) graph creates a signature that can be used to identify the type of vehicle. The simulations provided do not account for the slight mutual inductance of a vehicle that is not covering any part of the loop. The measured inductance data was fitted with a polynomial curve to show this difference. The total change of inductance, however, was very accurate and displays the usefulness of this type of simulation. The simulation and testing should provide a solid background of information for this research in the future.

The simulation also shows the need for a better method of data acquisition before vehicle identification or speed detection can be researched. The simulation and manual data collection should be sampled at rate in excess of hundreds of measurements per second. This amount of detail or better should result in data more specific to the geometry of the ferromagnetic undercarriage of the vehicle.

REFERENCES

1. J.H. Kell, I.J. Fullerton, M. K. Mills, “*Traffic Detector Handbook*”, U.S. Department of Transportation Federal Highway Administration Office of Research and Development, 1990.
2. M. K. Mills, “Inductive Loop System Equivalent Circuit Model” *Vehicular Technology Conference of IEEE*, vol. 2, pp. 689-700, 1989.
3. F.W. Grover, *Inductance Calculations*, Dover Publications, Inc., 1946.
4. M. N. Sadiku, *Elements of Electromagnetics, Third Edition*. New York: Oxford, 2001.
5. Richard C Dorf, *The Electrical Engineering Handbook , Second Edition*. CRC Press IEEE press, pp. 29, 2000.
6. PATH – University of Berkeley, *California PATH - Partners for Advanced Transit and Highways*, <http://www.path.berkeley.edu/>

Appendix B

ILD Simulation User's Guide

James R. Riehl

Under the Supervision of

Stanley G. Burns

August 19, 2002

Overview

The ILD Simulation is intended to approximately model the behavior of an Inductive Loop Detector (ILD) as a vehicle passes over it. The hope was that, by using a quasi-static model of ideal current loops, the basic characteristics of a vehicle inductance signature could be reproduced, and the causes of variations in the signature analyzed. The ILD Simulation's MatlabTM interface takes input parameters for the dimensions of the vehicle and the computational accuracy. The primary output of the program is a plot of loop inductance over time, called the vehicle signature. There is also an option to plot the first derivative of the vehicle signature, which is the rate of change in loop inductance.

Theory

A typical ILD system consists of a 6' x 6' rectangular coil of wire, 2 to 4 turns, arranged parallel to the road surface and about one inch below ground. The leads of the loop are connected to some circuitry beside the road, which is used to detect changes in inductance. This hardware connects a capacitor to the loop under the road to form an LC circuit, and measures the resonant frequency of the circuit which is related to the inductance.

When a vehicle passes over the loop, there is a net decrease in loop inductance due to eddy currents induced in the vehicle's metal parts. The effect of the eddy currents on the inductance dominates over any increase in inductance caused by ferromagnetic metals in the vehicle. A vehicle placed over a loop in a static magnetic field would increase the inductance by increasing the magnetic permeability in the vicinity of the loop. However, the constantly changing magnetic flux caused by an alternating current source creates eddy currents in the vehicle.

In the course of this research project, I attempted to work out an electrodynamic model using the eddy current solver of Ansoft's Maxwell 3DTM. This finite element electromagnetic field modeling software seemed to be the most rigorous solution available and ideally could have provided a great deal of insight into the problem. However, this attempt failed due to the sheer amount of computation time that would be required to produce a smooth, high resolution vehicle signature. The challenge then is to develop a simplified model of the eddy current effect. One solution is to model the car as one or more infinitesimally thin conducting loops. This is the approach of the flux method, described below.

Flux Method

Several simplifying assumptions must be made in order to apply a basic quasi-static flux analysis of the loop-vehicle system.

1. Car can be modeled as a thin current loop
2. ILD is perfect conductor
3. Length of one side of loop \gg radius of wire

The basic two equations used for this method use the quantity of induced emf, ε , to relate the loop inductance, L , to the magnetic flux through the loop, Φ_B .

$$\varepsilon = L \frac{di}{dt} \quad \varepsilon = \frac{dN\Phi_B}{dt}$$

$$L \frac{di}{dt} = \frac{dN\Phi_B}{dt}$$

Integrating both sides results in

$$Li(t) = N\Phi_B(t) = N \int \vec{B}(t) \cdot d\vec{A} \quad \text{over surface bounded by loop}$$

$i(t)$ is the current through the loop at time t , and N is the number of turns in the loop.

The magnetic field is approximated using the Biot-Savart Law. Since $B(t)$ is proportional to $i(t)$, the $i(t)$ terms cancel out when calculating the inductance.

Use

Note: The ILD Simulation uses the following files: ILD.m, ILD.mat, carplot.m, Loop_Mutual.m, Qloop_Mutual.m, Bfield.m, mag.m, CarVerts.m, Loops.m, AddLoopVerts.m, biot.m, and biotquad.m. All of these files need to be located in the Matlab™ path.

Open Matlab™ 5.3. Type “ILD” and press enter. This loads the graphical user interface for the ILD Simulation with the default parameters. Now, click on RUN, and the default simulation will begin. Almost all parameters for the model can be adjusted from this window. Most of these inputs are straight forward, but following is an explanation of some of the inputs that are not.

Offset left/right

The point of view is from the driver of the car moving towards the loop. Since the car moves in the positive x direction on the diagram, left means $+y$, and right means $-y$. For a car that is 1.5 meters wide, an offset of 1.65 meters (half the car width + half the loop width = $.75 + .9 = 1.65$ m) will cause the car to pass just to the left of the loop. The right side of the car will pass directly over the left side of the loop.

Resolution/Speed

This input changes with respect to the x -axis setting (See Toggle X-axis). If the x -axis is position, the label reads “Resolution.” The resolution input sets the number of data points that will be calculated from the start to stop positions of the car model. If time is the x -axis, the speed input controls the number of samples assuming a constant sample rate

(Default sample rate is 9 ms, but this can be changed in carplot.m, under ‘Calculate Number of Samples’).

Integration Accuracy

The magnetic flux integral, $Li(t) = N\Phi_B(t) = N \int \vec{B}(t) \cdot d\vec{A}$ is approximated by numerical computation. Given an integration accuracy input of N, the loop through which the flux is being approximated is divided into N^2 rectangles. The magnetic flux through each of these smaller rectangles is calculated at the center and assumed to be constant over the rest of the rectangle. The accuracy increases with N, but the computation time also increases by the square of N.

Start Position / Stop Position

In order to normalize the position inputs for different car lengths, the start and stop positions refer to the number of (car + loop) lengths. The car just begins to pass over the loop at 0, and is completely clear of the loop at position 1. The normalized position multiplied by the (car length plus loop length) equals the position in meters, where the car just begins to enter the loop at 0 meters.

Toggle X-axis

This button toggles the x-axis setting between

1. normalized position
2. position in meters
3. time in seconds

View Magnetic Field

Clicking this button will load a vector plot of the magnetic field and a shaded magnitude plot. The field will be calculated for whichever type of loop is selected, Rectangular, or Quadrupole. The code for the field calculations are located in biot.m, and biotquad.m, respectively.

Adding Additional Loops to the Car Model

To add additional loops to the car model, you will need to edit the code of carplot.m. In the Matlab command window, type “edit carplot”. The Matlab editor window will open. Scroll down to the “Additional Loops” heading. Determine the number, dimensions and location of any loops you would like to add, and insert a column for each additional loop.

Figure 1: Matlab Code Diagram

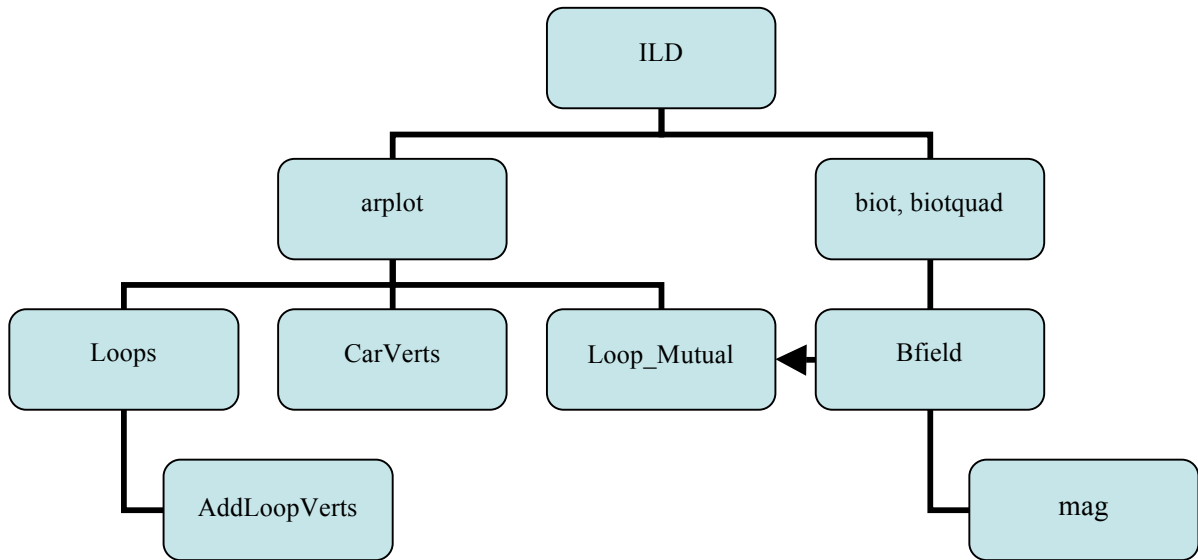


Figure 1 shows the organization of all the Matlab™ files needed to run the ILD Simulation. ILD is the main figure containing the user interface. From this interface, clicking “RUN” starts the carplot script. The functions CarVerts, Loops, and AddLoopVerts are simply used to calculate the 3D vertices of loops used in the model. These loops are used as inputs to the Loop_Mutual or QLoop_Mutual functions, depending on the type of loop selected, rectangular or quadrupole. These functions calculate the mutual inductance between two loops using Bfield, which computes the magnetic field using the Biot-Savart law. Finally, the mag function is simply used to take the magnitude of a vector.

Supplemental Functions

OffsetPlot.m, OffsetPlotQ.m

These functions generate a plot of peak inductance change vs. car offset for a rectangular, and quadrupole loop, respectively. Other parameters for the model are adjustable within the code for each function.

HeightPlot.m, HeightPlotQ.m

These functions generate a plot of peak inductance change vs. distance from car to ground for a rectangular, and quadrupole loop, respectively. Other parameters for the model are adjustable within the code for each function.

Discussion of Results

Using an extremely simplified model of the ILD/vehicle system, this simulation is able to fairly accurately predict the shape of a vehicle signature as well as the variations in the shape and intensity of the signature due to changing system parameters. However, it is difficult to reproduce the type of slight variations in signature that are observed in experimental ILD data.

Figure 2: Comparison of experimental (TOP) and simulated (BOTTOM) vehicle signatures.

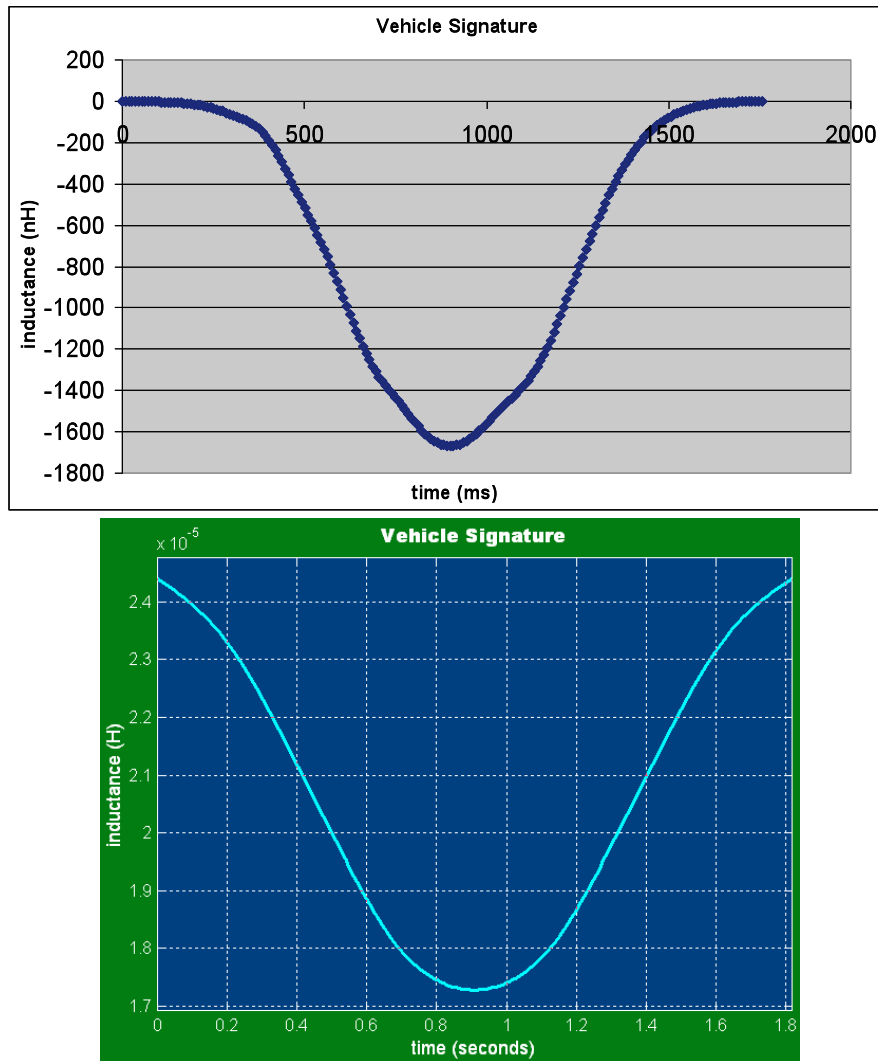
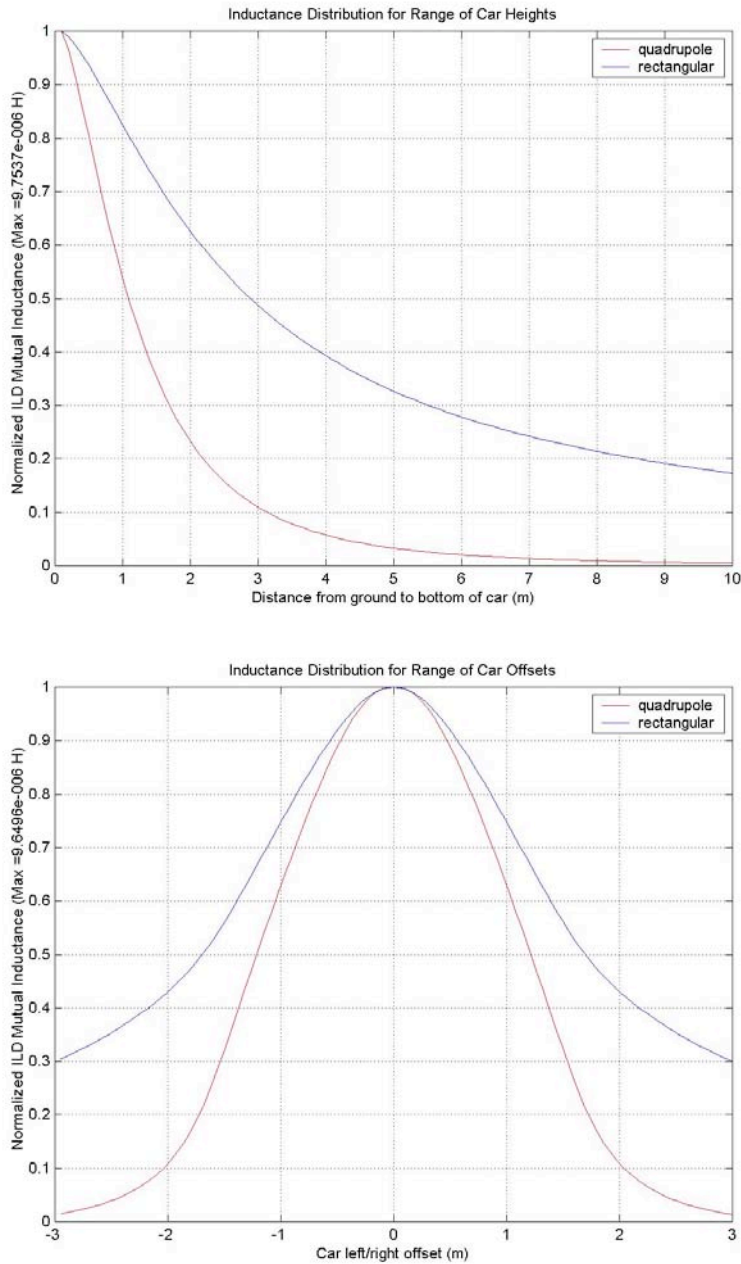


Figure 3 shows the sensitivity of the simulation. According to this model, a car in the next lane (~3m offset) of a rectangular loop would register about 30% of the peak inductance change of a car passing squarely over the loop. Also, a car traveling at four

meters off the ground would result in about 40% of the inductance drop of a car at ground level. The quadrupole loop shows somewhat less long range sensitivity.

Figure 3: Peak inductance change vs. car offset (top), car height (bottom)



Quadrupole Loop Model

There is some difficulty in using the loop car model with a quadrupole loop. If the same procedure is used for the quadrupole as for the rectangular loop, the total flux through the car loop would cancel out to zero over when the car is centered over the loop. This

occurs because of the opposing magnetic field directions on either side of the quadrupole loop. To get around this problem, instead of taking the net flux by summing the flux through each integration rectangle, the absolute value of the fluxes are summed to always give a positive total flux. This is analogous to modeling the car as a set of N^2 (where N is the integration accuracy) smaller loops of conducting wire. Some artefacts can be observed in the simulated quadrupole signatures.

Signal Processing

If the overall goal is to use the vehicle signatures to classify vehicles passing over the loop into categories, the best approach is probably to use a pattern recognition algorithm. The basic idea would be to extract a small number of features from the input signature, so each vehicle signature would be represented by a feature vector rather than a large data set. Then, the decision rules could be generated by using a training data set, where the classification of each vehicle is known and the feature vectors recorded. The crucial aspects of this processing are which features to use, and how to generate the decision rules. Oh, Ritchie, and Oh [1] achieved some success using the features, slope (“slew rate”) and duration, and implementing a probabilistic neural network for their classification method.

I made some attempts to analyze both the simulated and actual vehicle signatures in the frequency domain by taking a fast Fourier transform, but I did not observe any distinguishable features in the resulting plots. I was looking for some peak in the frequency spectrum that could be used to help classify different vehicle types. The following Matlab™ code will plot a power spectral density of a signature.

```
Y = fft(y), y is the input vector (inductance)
```

```
Pyy = Y.*conj(Y);
```

```
plot(Pyy);
```

Matlab™ files

Directory: C:\Documents and Settings\Administrator\My Documents\James ILD\ILDSim

ILD.m – ILD Simulation user interface figure

ILD.mat

carplot.m – starts when you click “RUN”, runs simulation

CarVerts.m – calculates vertices of car loop given dimensions, position

AddLoopVerts.m – calculates vertices of additional loops

Loops.m – combines all loops into a $4*N \times 3$ matrix

Loop_Mutual.m – rectangular loop mutual inductance

QLoop_Mutual.m – quadrupole loop mutual inductance

BField.m – magnetic field at a point due to a straight segment of current

mag.m – magnitude of a vector

Biot.m – generates vector B-field plot and shaded magnitude plot (rectangular)

Biotquad.m – generates vector B-field plot and shaded magnitude plot (quadrupole)

HeightPlot.m – plots peak inductance change vs. car height (rectangular)

HeightPlotQ.m – plots peak inductance change vs. car height (quadrupole)

OffsetPlot.m – plots peak inductance change vs. car offset (rectangular)

OffsetPlotQ.m – plots peak inductance change vs. car offset (quadrupole)

FeatureExtract.m – finds slope and duration of signature data [time column, inductance]

FeatureExtractSpline.m – finds same features using spline interpolation

Slope.fig – linearity of signature slope vs. speed using John's car data

LogDuration.fig -- linearity of log duration vs. speed using John's car data

SimLogDuration.fig – linearity of log duration vs. speed using simulated data

SimSlope.fig – linearity of slope vs. speed using simulated data

cardata.mat – John's car signature data

stratus.mat – James' car signature data

Recommendations for Future Work

I believe that the method of Oh and Ritchie could be improved upon by coming up with some more distinctive features of a vehicle signature. One possibility might be to simply use peak inductance change as a feature or the ratio of peak inductance to duration. These features should be affected by vehicle ground clearance, which is one more aspect that could be used to distinguish vehicle types. For a signal processing approach, however, it is very important to have a large amount of data, and right now, we do not have access to lots of data, so this is one obstacle that may need to be overcome before a signal processing approach can be seriously researched.

REFERENCES

Ritchie Oh. Real Time Traffic Measurement from Single Loop Inductive Signatures. *Institute of Transportation Studies*. University of California, Irvine. December 2001.

Appendix C

Inductive Loop Detector Simulation and Analysis

Prepared by

Vikram Gowreesunker

Under the Supervision of

Stanley G. Burns

August 26, 2003

Overview

I worked with the NATSRL from Spring 2002 to Summer 2003. Over this period, I took on several responsibilities related to the research of Inductive Loop Detectors (ILDs) and their improved application. Our long term goal was to be able to determine information other than simple presence of vehicles over the ILD. Our focus has been to determine the type of vehicle passing over the ILD and its possibly speed.

To this date, we have crossed a few milestones but are still not close enough to our long term goal. As detailed in this report, the different stages of my work involved:

1. setting up the equipment.
2. calibrate the equipment
3. simulate the magnetic field and inductance with MATHEMATICA™
4. Use Riehl's program to investigate some irregularities observed on the acquired data.

Besides the work mentioned above, I was involved in a few other facets of the research. I also worked with John Boeder in finding an appropriate DAQ board for the data acquisition. We also tried to use LABVIEW™ to process the acquired data.

Unfortunately, the LABVIEW™ experience was not very successful. I also tried to do some FFT operation on the data acquired through the 'Receive Delta' program. That was not very promising either, mainly because of its significant low sampling rate.

ILD Simulation using MATHEMATICA™

Below are excerpts from the senior project report of Zachary Gerbozy and Vikram Gowreesunker.

Abstract

Inductive loop detectors are used extensively in traffic control systems because of their high accuracy and non-intrusive characteristics. As a car passes over the loop its ferromagnetic undercarriage causes eddy currents to lower the inductance of the loop. The current application of the detector is to set a threshold for the change of inductance and thereby sense the presence of a vehicle. The purpose of this research project is to create a simulation of the continuous inductance change over time. This simulation was then compared with data collected from recently installed loop detectors at the NASTRL research facility. The resulting inductance information may lead to further identification of the vehicle being detected and single loop speed.

Introduction

Inductive loop detectors (ILDs) are a proven and effective method of vehicular detection in modern transportation systems. The data obtained from these devices has been found to be extremely accurate, highly reliable, and low-maintenance compared to other similar technologies. It is for this reason that the ILD is the most widely used detection method in modern traffic control systems. If it is possible to collect more information about the vehicles detected by an ILD, it could be obtained at a significant cost savings compared to another technology. Therefore, the purpose of our research is to simulate and verify the loop inductance as it changes when a vehicle passes over.

The inductive loop detector consists of a solenoid loop of wire buried underneath the pavement with the symmetric axis perpendicular to the road. The loop is connected via lead wire to an external circuit that measures its inductance. The loop is supplied with a low current source, which creates a magnetic field and self-inductance of the loop. When a vehicle with an undercarriage of mostly ferromagnetic material passes over the loop, it causes eddy currents to reduce the inductance of the loop [1]. The result is that the inductance of the loop is lowered and the detector counts the vehicle if that inductance change is greater than a certain threshold.

The basis for the computer simulation is to model the specific loops located at the NASTRL research facility. There are a total of four loops, three square loops and one quadrupole, made up of #12 AWG wire buried approximately two inches below the pavement. The loops are connected via pull boxes, which lead into the research facility and connect to the 3M Canoga C824T loop detector.

Equipment

The computer simulation was performed using the Mathematica 4.0 program. This software allowed the simulation to have an adequate balance between its high computational and graphical demands. Testing of the simulation required the installation of a 3M Canoga vehicle detection system. The NASTRL research facility had previously installed the loops below the adjacent pavement outside. The research team connected and successfully configured the following equipment to obtain data from the loops:

SOFTWARE

- ✓ Wolfram Research Mathematica 4.0
- ✓ 3M Canoga Model C800 Interface and Data Acquisition Software (C800IS)
- ✓ Camtasia 3.0.1 screen capture program

HARDWARE

- ✓ 1, 6' X 6' Square Loop (4 turns of #12 AWG wire)
- ✓ 1, 3M Canoga Vehicle Detector (C824T)
- ✓ 1, 3M Canoga Power Supply Unit (R124A)
- ✓ 1, RTC Detector Card Rack (CR54W)
- ✓ 1, 4' X 4' plywood mounting board
- ✓ 1, Gateway desktop computer
- ✓ 1, RS232 serial port cable

The power supply required a separate unit to safely connect the necessary 120 VAC to the card rack, which disperses 24 VDC to each of the four vehicle detector slots.

Methodology

As a preamble to the experiment, the magnetic field of a 1-turn 6x6 ft loop detector was simulated using Mathematica. The first step in this module was to derive the equation of the magnetic field. As shown in figure 1, loop is defined to be located on the $Z = 0$ plane in the first quadrant of the Cartesian coordinate system.

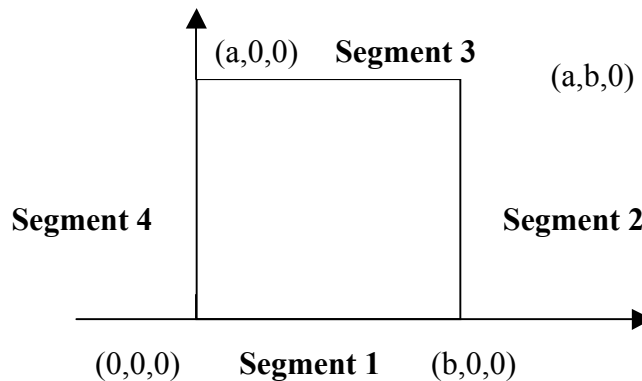


Figure 1. Diagram of Square Inductive Loop for Simulation

The loop is divided into 4 segments, and the magnetic field at a point in space from each isolated segment was computed by means of the Biot-Savart law. Therefore, the magnetic field B is defined by,

$$B = \mu * H$$

where

μ is the permeability of the material (H/m)

and

H is the magnetic field (ampere-turns/m).

Furthermore, the magnetic field for each of the line segments is independent. Using superposition, the corresponding vectors were added and displayed as a plot of the magnetic field surrounding the loop.

The inductance simulation requires the selection of a method of calculation as well as selection of specific equations to accurately model this parameter. The three primary methods of inductance calculations are LINK coupling coefficient, mutual coupling and NIWA current sheet of which the mutual coupling method is the most appropriate.

An outline of the mutual coupling method is given below.

- h) Computing external inductance of a wire segment [1]
- i) Generate equation to calculate Real and Imaginary Bessel functions and their derivatives. [2]
- j) Computing internal inductance of a wire segment using (b). [1]
- k) Compute total inductance of wire. [1]
- l) Computing the equation for Mutual Inductance between 2 parallel filamentary wires. [1]
- m) Use (c) to calculate the Mutual Inductance between 2 parallel rectangular loop. [1]
- n) Use (d) to compute the Mutual Inductance among the 4 parallel loops. [1]

A similar simulation for the self-inductance was also shown using a more basic method that does not incorporate the Bessel functions. A comparison between the two methods shows that there is a constant error in the self-inductance where the more advanced simulation is more accurate. The more important information, the change of inductance (ΔL), remains consistent through both simulations.

When a car passes over an ILD, an eddy current forms (due to the current through the loop) and a resulting self-inductance develops in the car. There are no specific formulas for the complex geometries of vehicles therefore we must use an approximation. The two main geometries that were considered were a current loop and a current sheet, each with dimensions similar to those of the undercarriage of the car. The sheet method prevailed because it was the easiest to model under the restrictions imposed by movement. The sheet formula used to calculate the inductance of a vehicle is,

$$L_{car} = (\mu * \mu_0 * h * x) / w.$$

Using this calculation,

$\mu * \mu_0$ is the permeability of the pavement (in H/m),

h is the height of the car above the loop (in meters),

w is the width of the car (in meters),

and x is the length of the vehicle covering the loop (in meters).

With the sheet method, the effective inductance of the vehicle changes as more or less of the vehicle covers the loop. This simplification is not possible with the loop method and therefore it was not practical to use.

The final aspect of the inductance calculation is the mutual inductance equation.

The basic equation for mutual inductance between two circuits is,

$$M_{12} = k * (L_1 * L_{car})^{1/2},$$

where k is the coupling coefficient. The resulting total inductance of the loop is then calculated by the formula,

$$L_T = L_1 - M_{12}$$

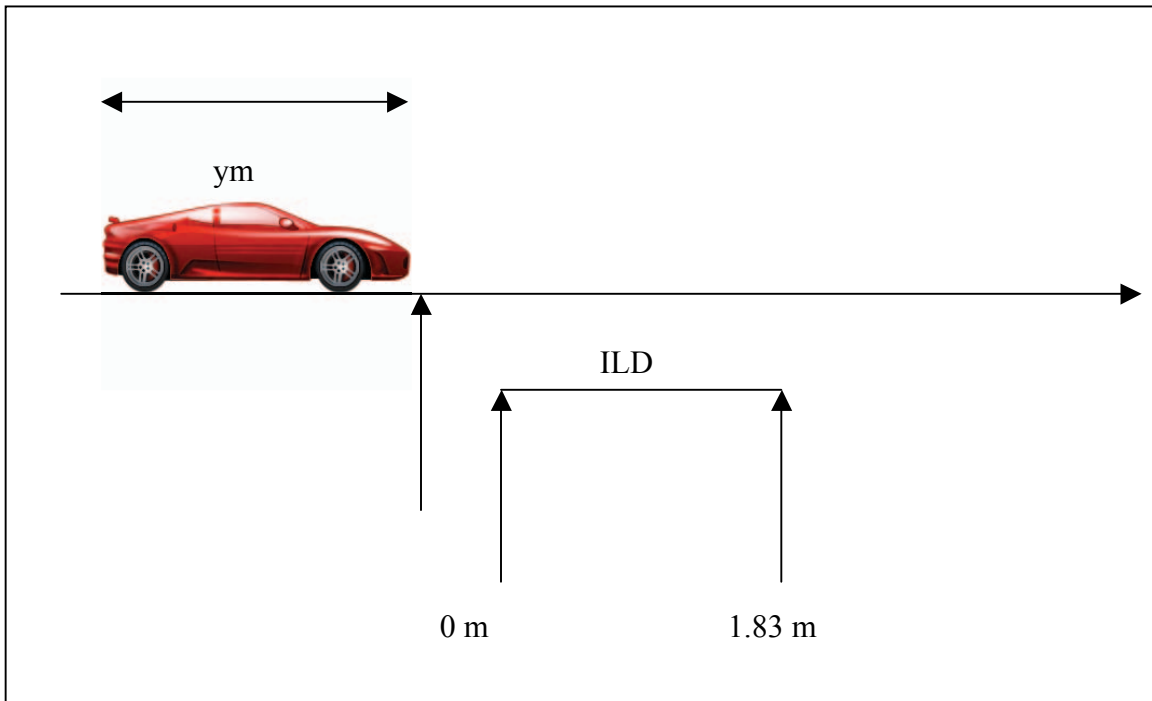


Figure 2. Diagram of Vehicle Position for Inductance Simulation

Since the equation for the inductance of the vehicle (L_{car}) is only non-zero when some of the vehicle is over the loop, the mutual inductance is only valid under this condition. Figure 4 shows the relative positions of the loop detector and vehicle for the simulation.

Results

The simulation of the magnetic field verified the information given by the literature in showing that the field is strongest in the center of the loop. Figure 2 shows the vector plot simulation of a six-foot square loop.

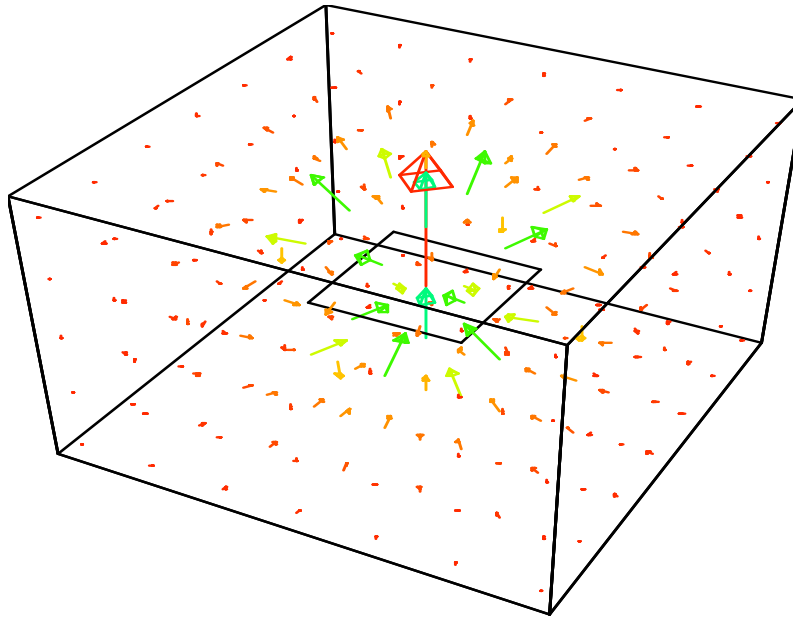


Figure 3. Magnetic Field Simulation of a Square Loop

The magnetic field lines follow the right hand rule corresponding to a counter-clockwise current flowing through the loop. The difference in colors and length show the intensity of the field lines is strongest in the center and decays exponentially away from the loop.

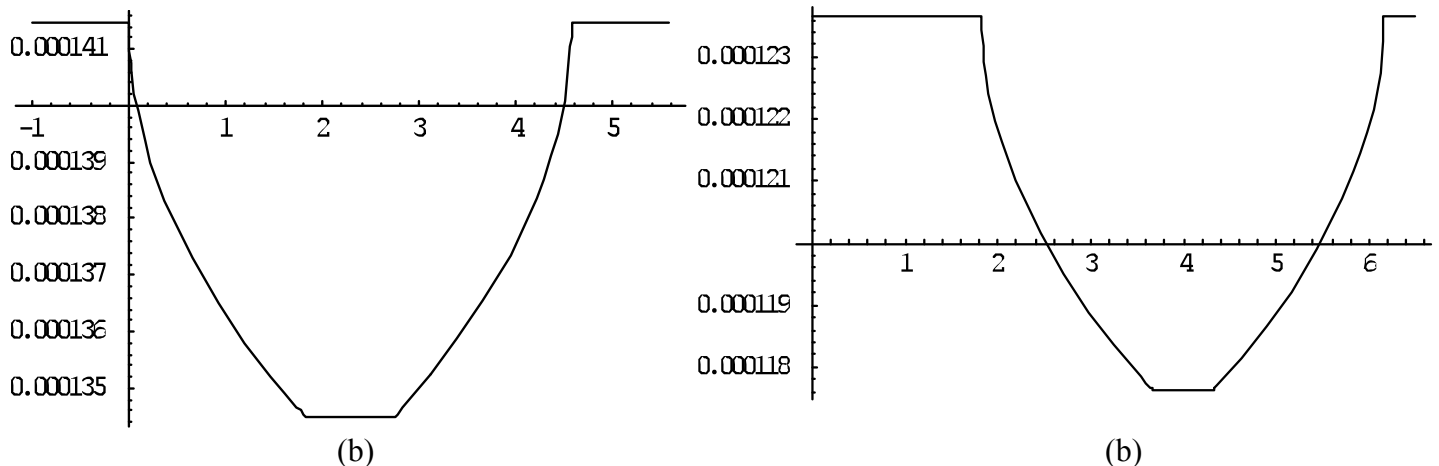


Figure 4. (a) Basic Inductance Simulation (b) Advanced Inductance Simulation

Discussion

The results of our research show the inductance vs. distance (time) plot for a vehicle and the supporting simulation of this event. This plot can be thought of as a signature for a particular type of vehicle traveling at a certain speed. This information could lead to a more advanced model of traffic flow utilizing the existing technology. In order to successfully develop these models, however, research would need to be conducted develop these signatures more quickly, accurately, and easily.

Data acquisition research for the inductive loop detectors could be approached from either an analog or a digital perspective. The analog approach to obtaining these signatures would involve the purchase of a frequency to voltage converter applied to the outputs of the inductive loop. Recording these signatures is possible using Labview, however, it would require a detailed schematic of the circuitry of the loop detector. Another approach would be to analyze the digital information sent by one of the Canoga C800IS software programs, which displays the real-time inductance data. A simple Visual Basic program could capture and show this data, however, a more detailed understanding of the software program is required for this approach.

Following a data acquisition project, a research team could extensively test different vehicles to obtain signatures for analysis. These signatures could be used possibly with a fuzzy logic control package to deliver the vehicle type information along with the vehicle count. Speed detection from a single loop is also possible through advanced algorithms for determining the vehicle length.

Conclusion

The research shows the possibility to obtain more information from the inductive loop detector. The inductance versus time (or distance) graph creates a signature that can be used to identify the type of vehicle. The simulations provided do not account for the slight mutual inductance of a vehicle that is not covering any part of the loop. The measured inductance data was fitted with a polynomial curve to show this difference. The total change of inductance, however, was very accurate and displays the usefulness of this type of simulation. The simulation and testing should provide a solid background of information for this research in the future.

The simulation also shows the need for a better method of data acquisition before vehicle identification or speed detection can be researched. The simulation and manual data collection should be sampled at rate of at least 1000 measurements per second. This amount of detail or better should yield data more specific to the geometry of the ferromagnetic undercarriage of the vehicle.

Receive Delta Program

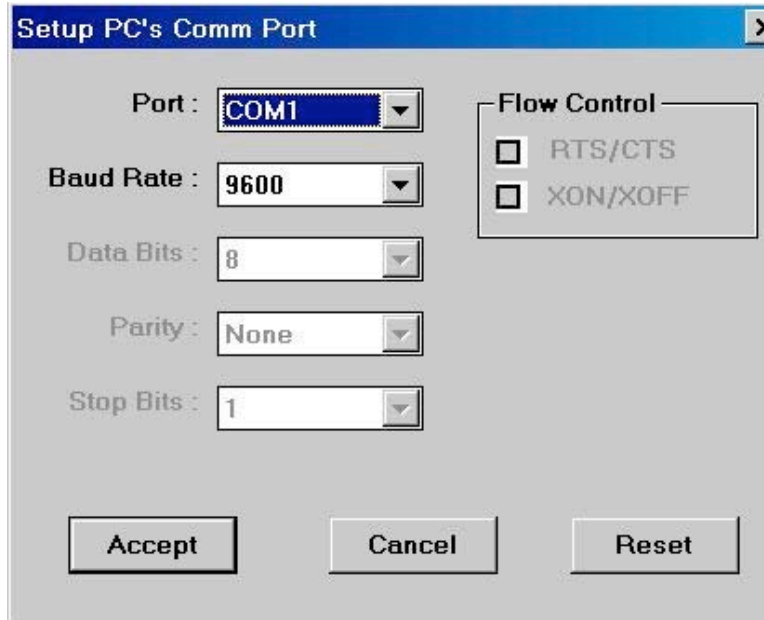
Data Collection from ILDs using the ReceiveDelta Program

The Receive Delta program works with the Canoga system to sense inductance changes of Inductive Loop Detectors, installed at the I-35 site.

How to use the Receive Delta Program?

- (1) The Canoga system must be connected correctly. That is, if loops 2 and 3 are to be sampled, then these 2 loops must be wired to the Canoga. Then, the serial cable of the Canoga must be connected to one of the Com ports of the PC (we selected com port 1).

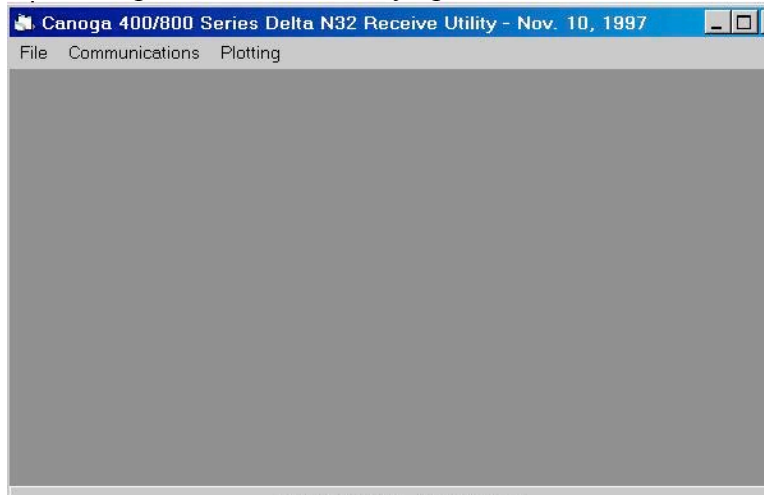
- (2) The sensitivity levels of the loops are set using the Canoga board. In this test, sensitivity 4 was picked for loop2 and sensitivity 2 was picked for loop3.
- (3) The program is started and the first window that opens is the configure window. Here, the settings are defined.



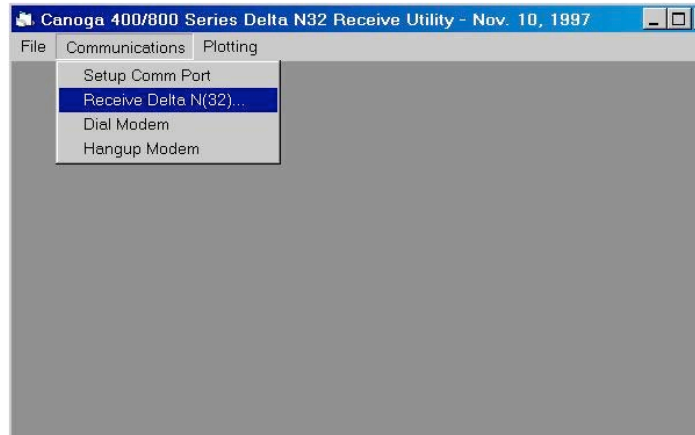
Com port number = 1

Baud rate = 9600

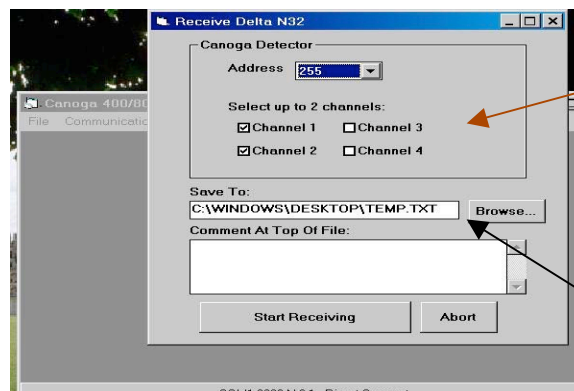
- (4) After the settings are chosen, click “Accept”. The status bar of the Receive Delta should show that the port was successfully opened.



- (5) Click on ‘Communications’, then ‘Receive Delta N(32)’ from the drop down menu as illustrated below.



(6) The following window appears:



Choose the channels to sample. Max of 2

Remember to

Click 'Start Receiving' to start collecting data.

(7) Status window will pop-up. It looks as follows:



(8) Click on 'Stop' to stop collecting data.

(9) The 'status' window (step 7) and 'Receive Delta' window (step 6) will disappear.

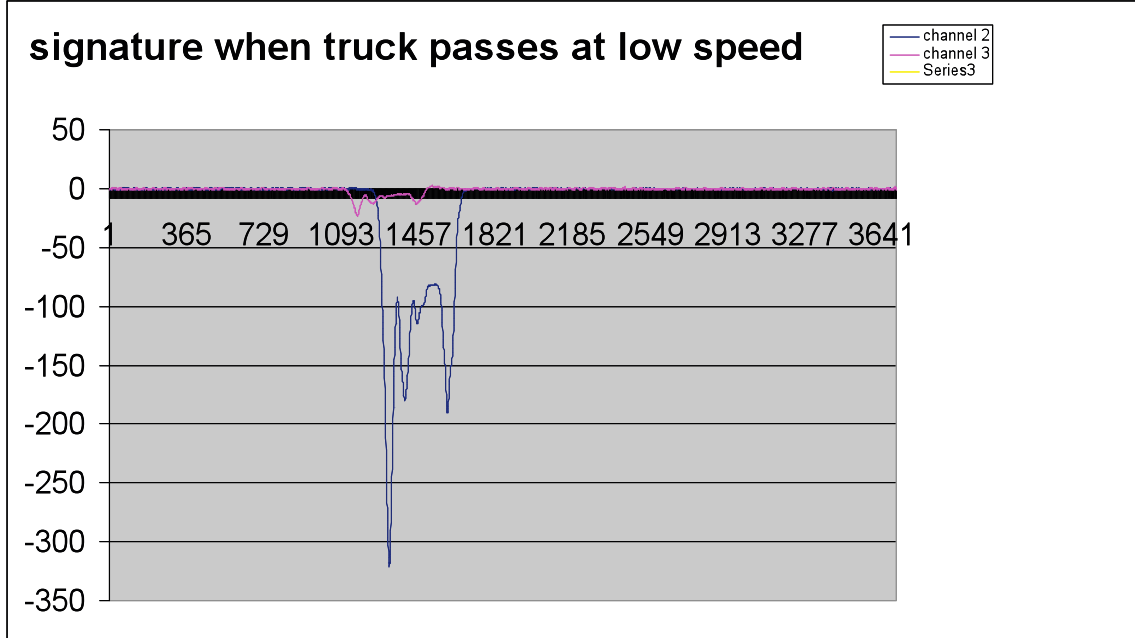
(10) A text file containing the data will be created at the location that was chosen in step 6.

Experiments & Results

The data collected by the program is stored in a text file. The text file can be formatted by Microsoft Excel for graphical interpretation.

Example 1 - truck

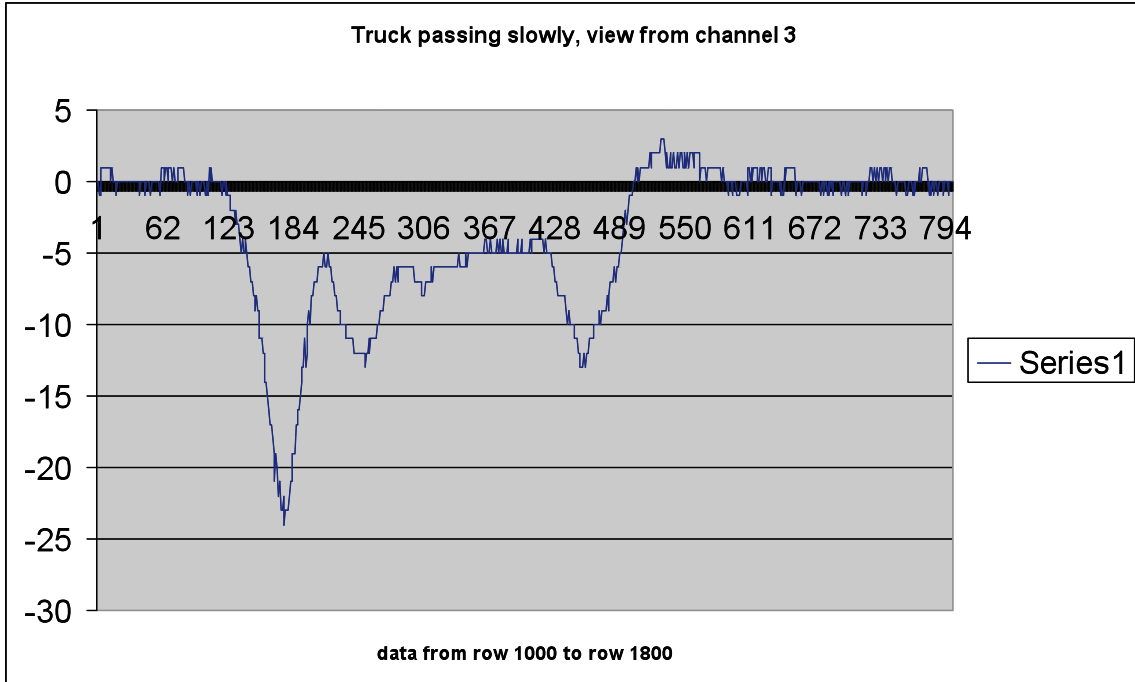
For example, the data collected for a truck passing slowly over the ILD 2 and ILD 3 are documented in the “truck.txt” file. The same data was extracted to an excel file for graphical display and ease of manipulation.



As seen above, both channel 2 and 3 have more or less the same shape. However, channel 2, which was set a higher sensitivity, has a more intense curve.

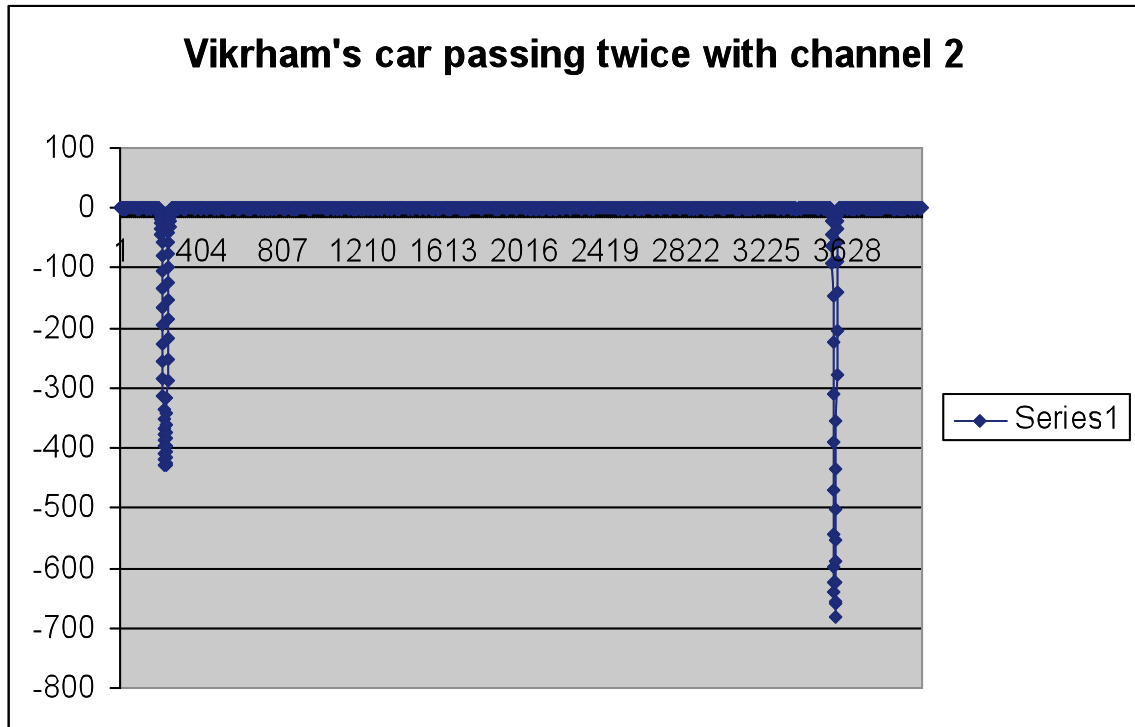
In the figures below, the two curves have been isolated and zoomed in appropriately.

Channel 2 was at sensitivity level 4.

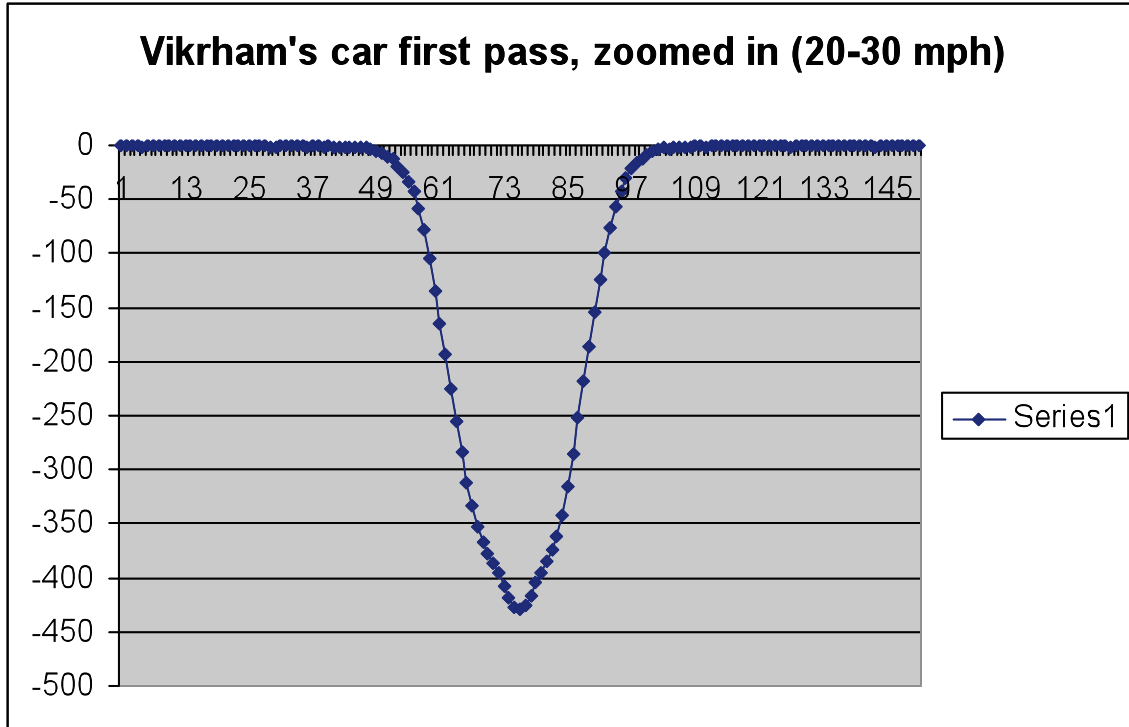


Channel 3 was at sensitivity level 2. Compare the y-axis scale with respect to the previous graph. One can notice that the intensity is distinctive less.

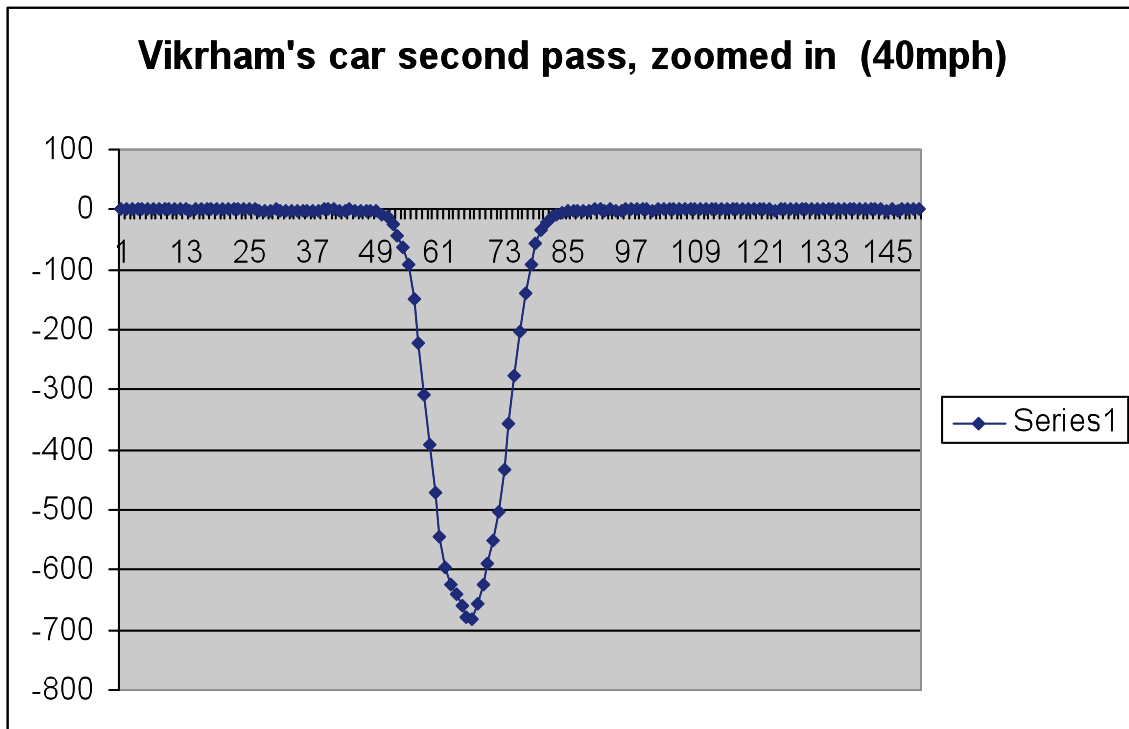
Example 2 – Pontiac Grand Am 91.



As seen above, there are two distinct dips in the inductance levels. The second one is significantly deeper. The second pass was at least 10 mph faster.



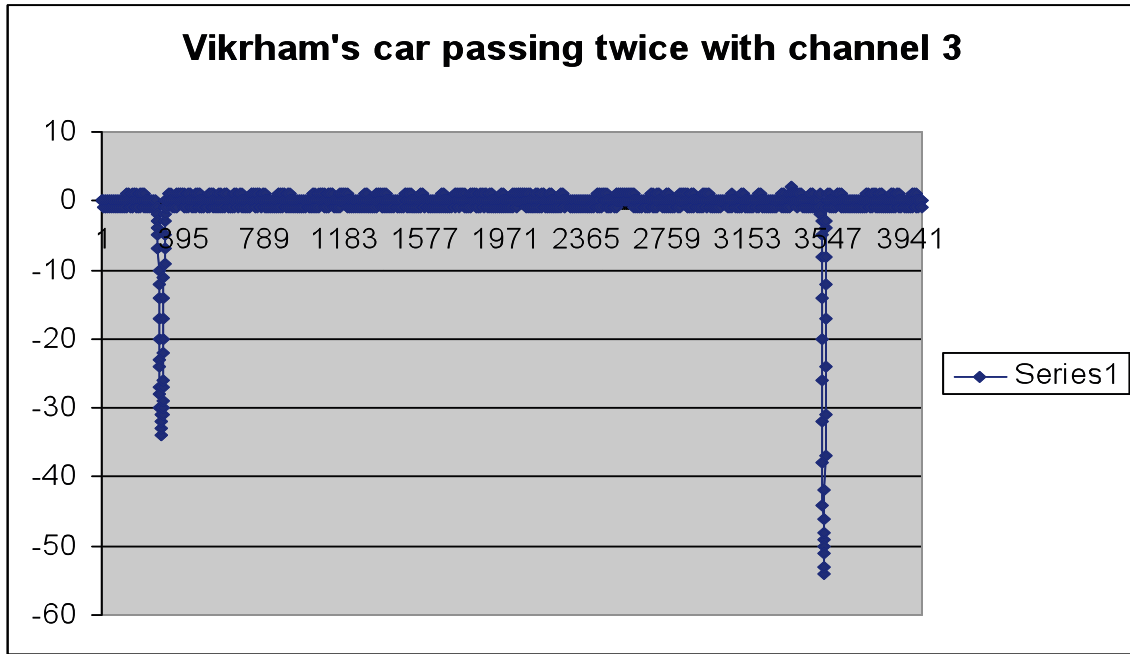
From the above graph, we notice that the maximum change in inductance = 425, while the width of the dip is about 50 units.



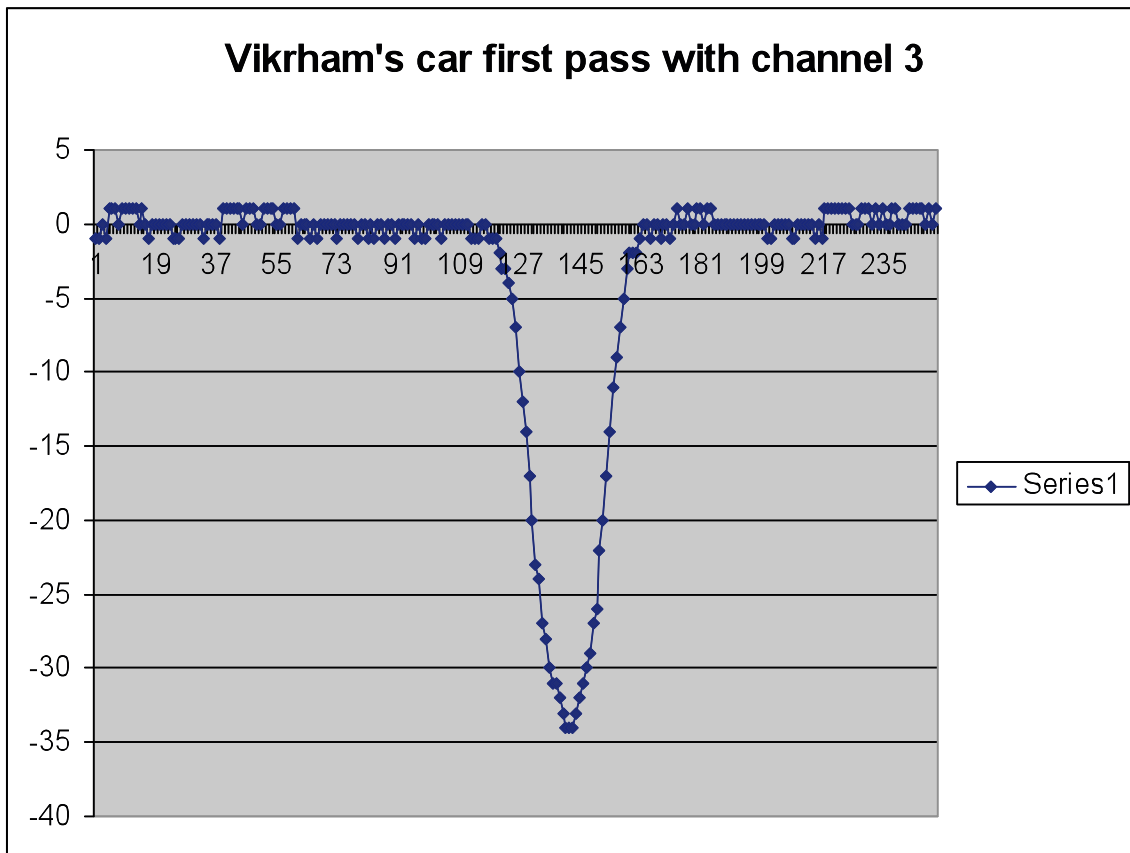
From the above graph, we see that the maximum dip = 700, while the width of the dip = 36.

Example 2 (contd)

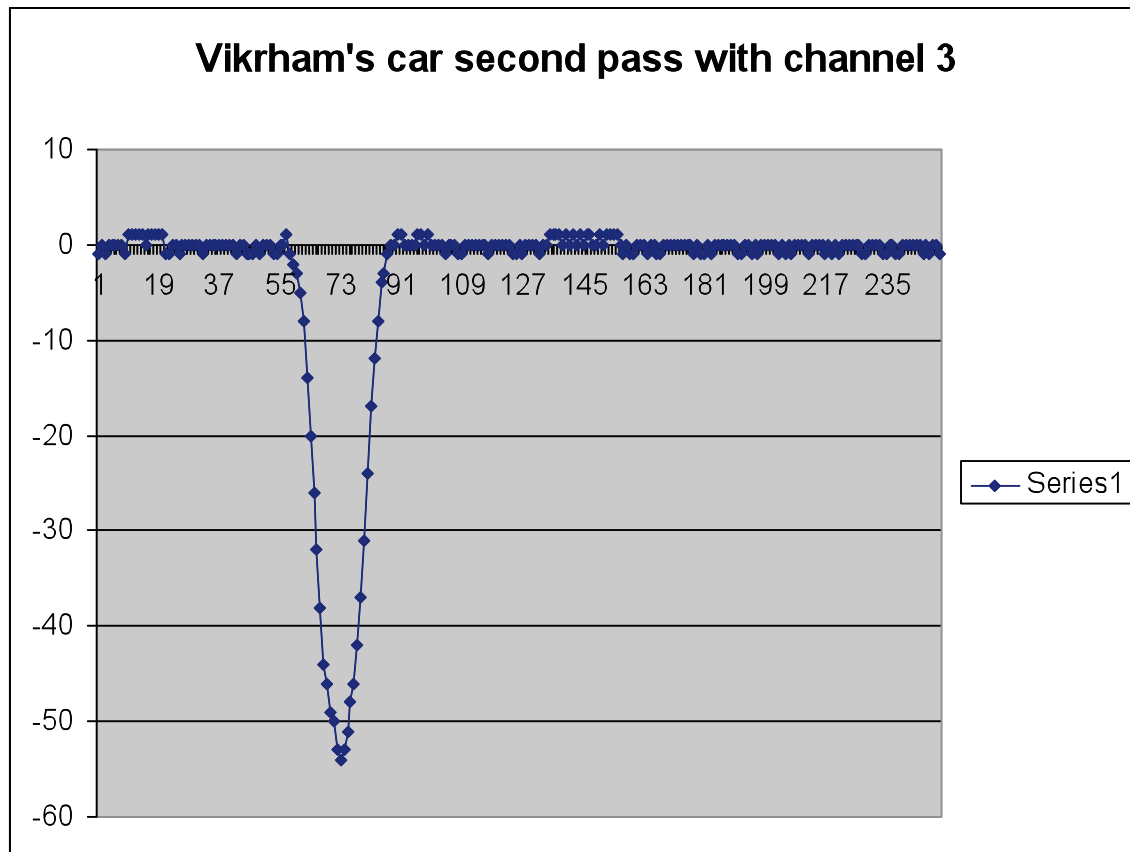
The same data was also recorded using ILD 3, i.e. channel 3.



Above, we notice the same pattern as for channel 2, with 2 dips and the second one significantly deeper.



From the above graph, we notice that the maximum change in inductance = 34, while the width of the dip is about 36 units.



From the above graph, we notice that the maximum change in inductance = 55, while the width of the dip is about 37 units.

Interpretation

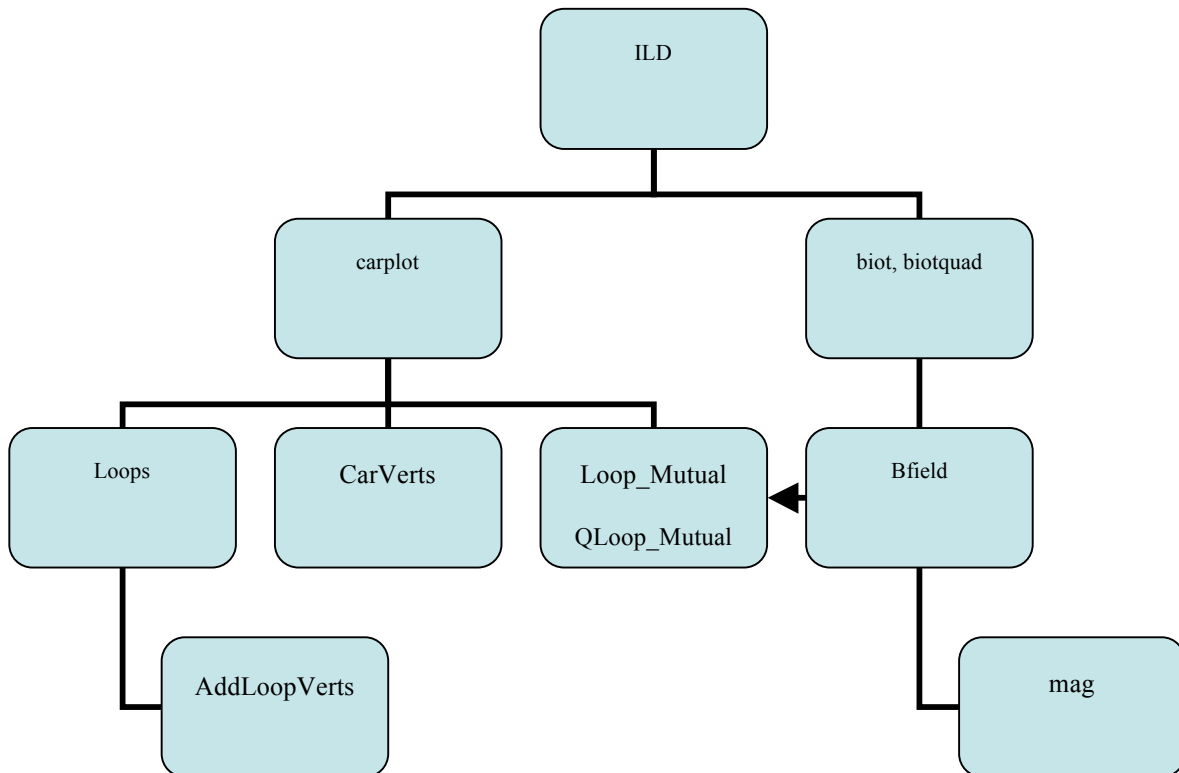
The initial testing shows a distinct difference in the intensity and quality of the curves obtained with different sensitivities. Other differences include:

- We also notice a difference in graph shape between a car and a truck
- There is also a difference in width and length of the curve with various speeds.

James Riehl 's Matlab program

Quoting James Riehl's Report [5], "The ILD Simulation is intended to approximately model the behavior of an Inductive Loop Detector (ILD) as a vehicle passes over it. The hope was that, by using a quasi-static model of ideal current loops, the basic characteristics of a vehicle inductance signature could be reproduced, and the causes of variations in the signature analyzed. The ILD Simulation's Matlab™ interface takes input parameters for the dimensions of the vehicle and the computational accuracy. The primary output of the program is a plot of loop inductance over time, called the vehicle signature. There is also an option to plot the first derivative of the vehicle signature, which is the rate of change in loop inductance."

The files are organized as follows [5] :



Using Riehl's program

1. All the files should be in the same folder.
2. Change the Matlab working directory to the folder in question.
 - a. For example if the files are in a folder **ILD**, in the C drive.
 - b. Change the directory by writing “cd C:/ILD”
 - c. Now we are ready to work.
3. From the Matlab command window, type **ILD**. A GUI window will appear.
4. The window looks like the following image.
5. The window is an interactive one with several options to customize the type of **ILD**, vehicle type and position. Details of the options and their meaning can be found in J.Riehl's report [5]. Below is an excerpt of the description.

Offset left/right

The point of view is from the driver of the car moving towards the loop. Since the car moves in the positive x direction on the diagram, left means +y, and right means -y. For a car that is 1.5 meters wide, an offset of 1.65 meters (half the car width + half the loop width = $.75 + .9 = 1.65$ m) will cause the car to pass just to the left of the loop. The right side of the car will pass directly over the left side of the loop.

Resolution/Speed

This input changes with respect to the x-axis setting (See Toggle X-axis). If the x-axis is position, the label reads “Resolution.” The resolution input sets the number of data points that will be calculated from the start to stop

positions of the car model. If time is the x-axis, the speed input controls the number of samples assuming a constant sample rate (Default sample rate is 9 ms, but this can be changed in carplot.m, under ‘Calculate Number of Samples’).

Integration Accuracy

The magnetic flux integral, $Li(t) = N\Phi_B(t) = N\int \vec{B}(t) \cdot d\vec{A}$ is

approximated by numerical computation. Given an integration accuracy input of N, the loop through which the flux is being approximated is divided into N^2 rectangles. The magnetic flux through each of these smaller rectangles is calculated at the center and assumed to be constant over the rest of the rectangle. The accuracy increases with N, but the computation time also increases by the square of N.

Start Position / Stop Position

In order to normalize the position inputs for different car lengths, the start and stop positions refer to the number of (car + loop) lengths. The car just begins to pass over the loop at 0, and is completely clear of the loop at position 1. The normalized position multiplied by the (car length plus loop length) equals the position in meters, where the car just begins to enter the loop at 0 meters.

Toggle X-axis

This button toggles the x-axis setting between

4. normalized position
5. position in meters
6. time in seconds

View Magnetic Field

Clicking this button will load a vector plot of the magnetic field and a shaded magnitude plot. The field will be calculated for whichever type of loop is selected, Rectangular, or Quadrupole. The code for the field calculations are located in biot.m, and biotquad.m, respectively.

[Running the Program

To run the program, click the RUN button.]

Editing Riehl’s Program

The most important file is the carplot.m. The file basically combines all the other files and relates them to the GUI figure. When the “RUN ” button is clicked, the values on the GUI window are loaded onto the carplot.m file. Carplot.m will use these initial values and some of the other files in the folder to compute Inductance and Change of Inductance. These quantities will be plotted on the GUI as the car position changes.

Most changes that might need to be done will require modifying the carplot.m file.

Adding Additional Loops to the car model

To add additional loops to the car model, one needs to modify the carplot.m file. On line 71 of the file, there are instructions on how to add more loops.

Files Description - Below is how J.Riehl describes the files:

ILD.m – ILD Simulation user interface figure

ILD.mat

carplot.m – starts when you click “RUN”, runs simulation

CarVerts.m – calculates vertices of car loop given dimensions, position

AddLoopVerts.m – calculates vertices of additional loops

Loops.m – combines all loops into a $4*N \times 3$ matrix

Loop_Mutual.m – rectangular loop mutual inductance

QLoop_Mutual.m – quadrupole loop mutual inductance

BField.m – magnetic field at a point due to a straight segment of current

mag.m – magnitude of a vector

Biot.m – generates vector B-field plot and shaded magnitude plot (rectangular)

Biotquad.m – generates vector B-field plot and shaded magnitude plot (quadrupole)

HeightPlot.m – plots peak inductance change vs. car height (rectangular)

HeightPlotQ.m – plots peak inductance change vs. car height (quadrupole)

OffsetPlot.m – plots peak inductance change vs. car offset (rectangular)

OffsetPlotQ.m – plots peak inductance change vs. car offset (quadrupole)

FeatureExtract.m – finds slope and duration of signature data [time column, inductance]

FeatureExtractSpline.m – finds same features using spline interpolation

Slope.fig – linearity of signature slope vs. speed using John’s car data

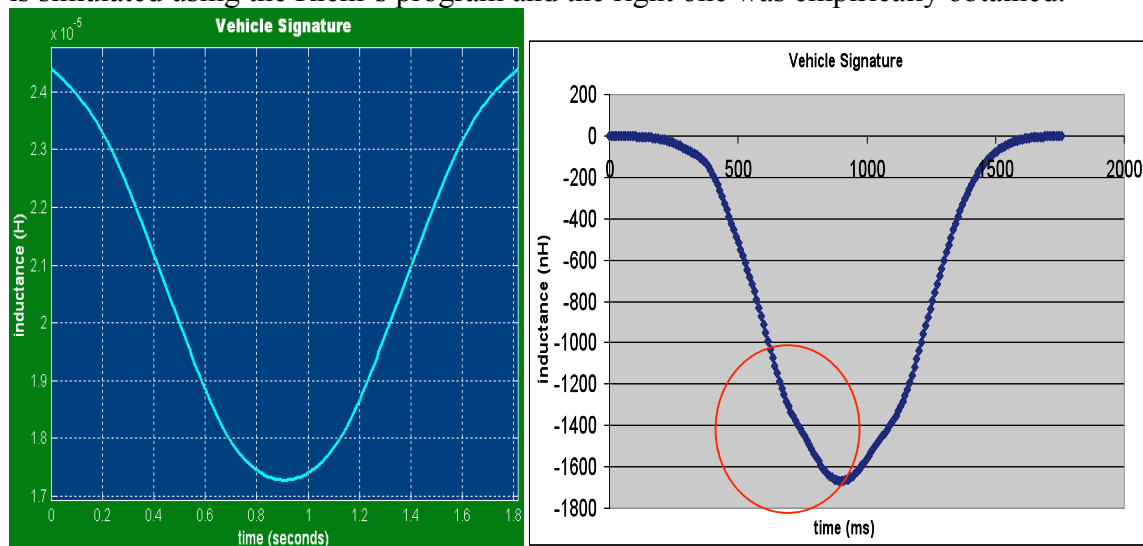
LogDuration.fig -- linearity of log duration vs. speed using John’s car data

SimLogDuration.fig – linearity of log duration vs. speed using simulated data

SimSlope.fig – linearity of slope vs. speed using simulated data

MODIFICATION AND ANALYSIS OF RIEHL’S PROGRAM

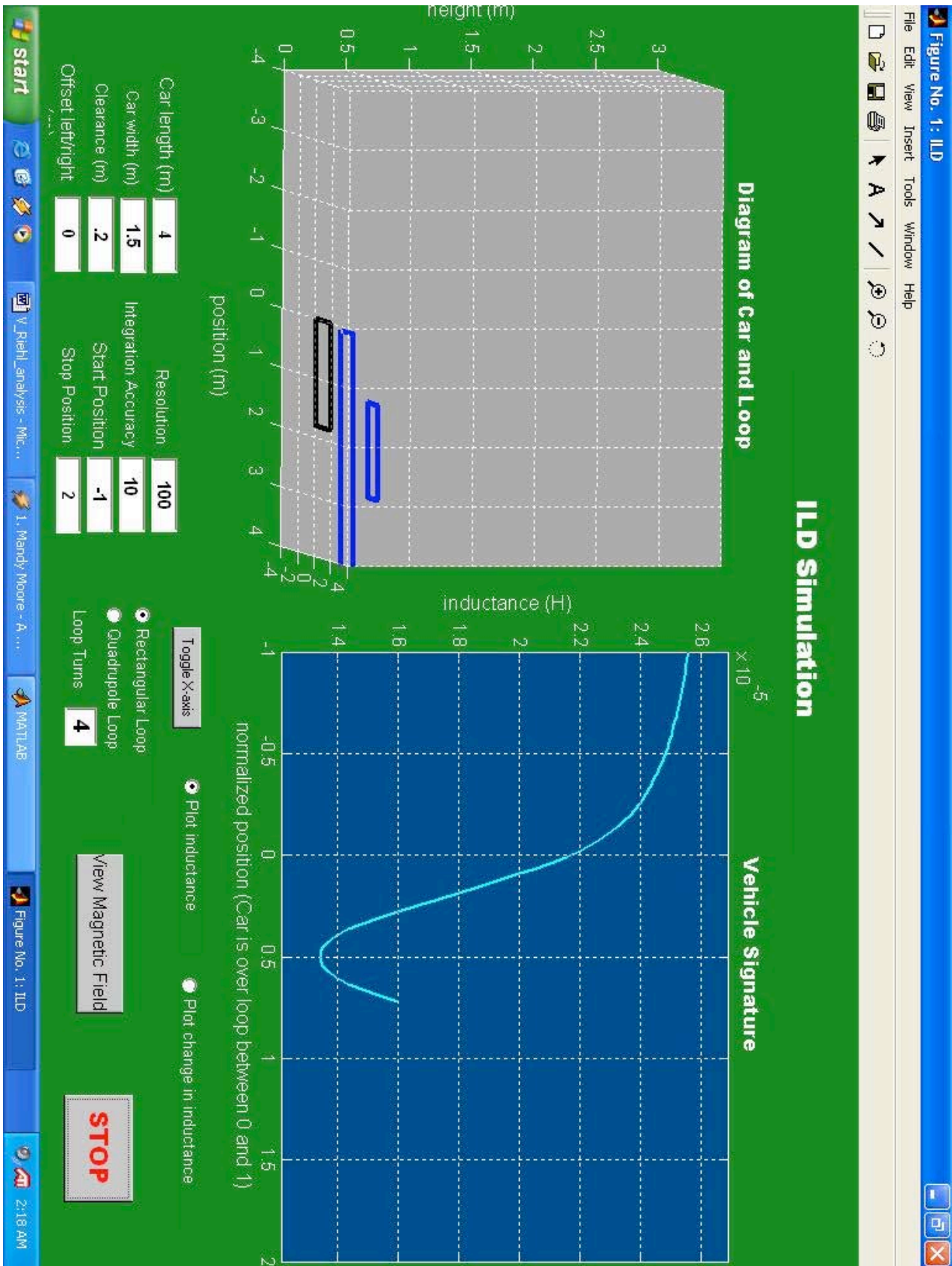
Riehl’s program was designed for simulating Inductance change as a vehicle goes over the ILD. The program included some provisions for altering the design of car by adding new loops. Empirical data showed one very interesting observation for the signatures of cars. The acquired curve was not as perfect as that of the simulated curve. More specifically, one very distinct structure could be observed. Below are two curves, the left is simulated using the Riehl’s program and the right one was empirically obtained.



As seen from the image on the right hand side, the curve has a small irregularity. It was originally assumed that it might be cause due to the axles of the vehicle. To verify this theory, we simulated the two axles of the car as two loops using Riehl's program. The program was run and compared to the model without the axle. Below is an account of what we found.

First, the program was run for a generic car (modeled as two loops – undercarriage and dome). The simulation is shown on the following image.

Figure No. 1: ILD



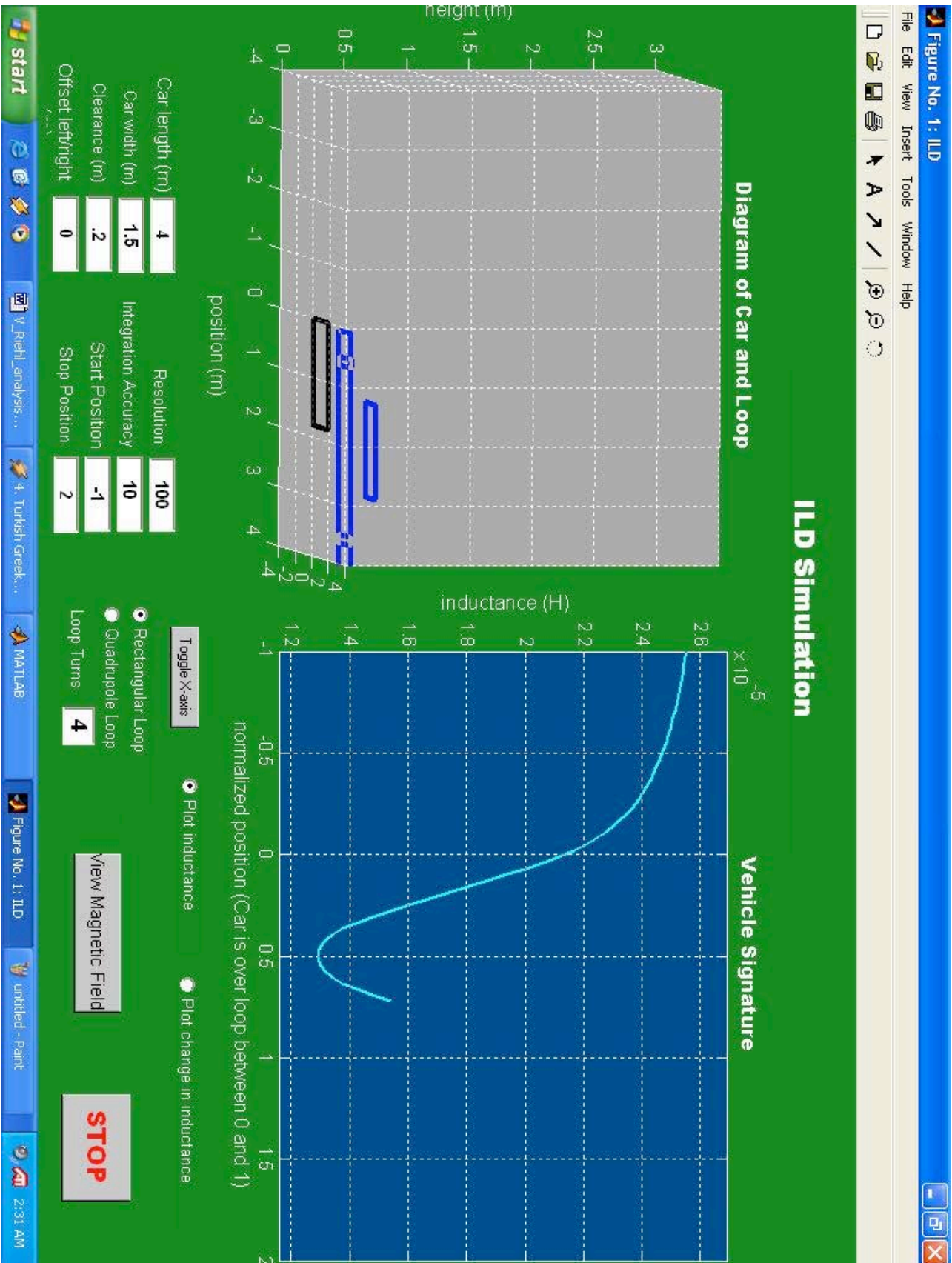
Next, we change the “carplot.m” file and added two loops to model the axles. Below is the portion of the code that was modified.

Original Code	New Code
<pre> %-----% %-----ADDITIONAL LOOPS-----% % Enter the following dimensions of each loop relative to the size of the car loop xL = [0.4]; % [Loop1 Loop2 Loop3 LoopN] xW = [0.8]; %1= same width as car xH = [0.2]; %1 = same height as car (+/- m) xPosX = [0.5] % 0.5 = centered in X of car xPosY = [0.5] % 0.5 = centered in Y of car </pre>	<pre> %-----% %----ADDITIONAL LOOPS-----% % Enter the following dimensions of each loop relative to the size of the car loop xL = [0.4 0.0375 0.0375]; xW = [0.8 1 1]; xH = [0.2 0 0]; xPosX = [0.5 0.125 0.875]; xPosY = [0.5 0.5 0.5]; </pre>

As it can be observed from the table above, all that needs to be done to add a loop to the car model is add a new dimension to the matrices of xL, xW, xH, xPosX and xPosY.

In the following figure, we see the differences when two new axles are added in the form of 2 loops.

Figure No. 1: ILD



As it can be observed from the two graphs, the actual structure of the curve does not change when the axles were added. We experimented with different axle positions and the results were not very promising. The only noticeable changes were (1) the drop in inductance increased and (2) the slope appeared to have changed.

Although the outcome of this theory was a little bit of a disappointment, we found another plausible explanation to the phenomenon. The hypothesis is that the irregularity is caused by the mass of the engine.

Postulate: The irregularity is caused by mass of engine, not axles or other fine car structure.

Reasoning: The structure shows that there is sudden change of pattern in the way the inductance decrease occurs when the car passes over the ILD. In fact, it looks like the decrease is considerably slowed down at some point.

There is a possibility that the mass of the engine causes a significant increase in permeability. Since inductance of the system decreases with increase in permeability, we could attribute that curve irregularity to the engine.

Verification: It was very hard to verify this theory with the current program. The design does not allow for change of permeability in only one section of the car. As a result, I would recommend writing a different program to simulate that.

Conclusion

Although the research has not reached its peak yet, I believe that we have made substantial progress. Most of the small details have now been taken care of and we are almost ready to start collecting some serious data. In terms of simulation, I believe that we have to find a way to simulate the different magnetic permeability of the vehicle's engine. This could involve some intense programming and substantial electromagnetic calculation. However, the results could be very interesting.

My experience with NATSRL has been a memorable one. I got the opportunity to work in every aspect of Electrical and Computer Engineering: simulation, mathematical derivations, on-site wiring diagrams and data acquisition. Nothing else could have prepared me better for graduate school and future industry work.

My only regret is that I never got to reach the stage where we could do some good signal processing on the data. But after this summer, the data should be available to work with.

REFERENCES

1. J.H. Kell, I.J. Fullerton, M. K. Mills, "*Traffic Detector Handbook*", U.S. Department of Transportation Federal Highway Administration Office of Research and Development, 1990.
2. M. K. Mills, "Inductive Loop System Equivalent Circuit Model" *Vehicular Technology Conference of IEEE*, vol. 2, pp. 689-700, 1989.

3. F.W. Grover, *Inductance Calculations*, Dover Publications, Inc. Mineola, NY, 1946.
4. M. N. Sadiku, *Elements of Electromagnetics, Third Edition*. New York: Oxford, ch. 8, 2001.
5. J. Riehl, "ILD Simulation User Guide" August 19 2002.
6. Ritchie Oh. "Real Time Traffic Measurement from Single Loop Inductive Signatures," *Institute of Transportation Studies*, University of California, Irvine. December 2001.

Appendix D

An Overview of Using Magneto-resistive Sensor Arrays For Traffic Measurements

by

Stanley G. Burns and Timothy Delf

Overview

In-situ vehicle occupancy, vehicle type classification, and speed are important measurements needed in traffic management. Most operational methods rely on threshold set inductance changes in the standard 6 foot square inductive loop detector augmented by limited use of video cameras and associated image processing. Typically, vehicle occupancy is determined by exceeding an eddy current induced inductance change threshold at a given ILD location. However, if one examines analytically and experimentally the time-dependent inductance change profile rather than the threshold switching level for establishing an occupancy number, there are unique signatures associated with different vehicle types. There appears to be correlation with vehicle structure both experimentally and in simulations, however it is clear that the ILD large size, system sample rate, and the vehicle speeds precludes the differentiation needed for the numerous NHTSA classifications although major classes can be identified. Basically, the ILD can not be treated as an spatial zero-width impulse sampled-data response system, which implies the spatial resolution is not adequate for vehicles moving at normal speeds.

Buried magneto-resistive sensors potentially offer another approach to obtain this traffic management data. The magneto-resistive sensor is a sensitive three-axis magnetometer with in-situ correction for the net vector magnitude 0.5 G Earth's magnetic field. The magnetometer responds to the local magnetic field perturbations resulting from the relative permeability change, m_r , of ferrous vehicle subsystems passing over the sensor such as the frame and engine. The essentially point source nature of the magneto-resistive sensor with a 6 ms sampling time whose active sensing dimension is on the order of 2 cm results in 3 inch spatial resolution of a vehicle traveling at 30 mph. Consequently, one is able to differentiate between different portions of a vehicle such as the engine, frame, and axles by measuring magnetic field deviations. An array of these sensors can then be used to provide a unique in-situ mapping of a vehicle configuration.

Approach And Analysis

The basic approach was to model and measure a vehicle-induced time-domain inductance change, when using an Inductive Loop Detector (ILD) and the localized magnetic field perturbation when using a magneto-resistive sensor and compare the results analytically and experimentally. Figure 1 is a schematic diagram of both sensing systems located at a test facility, Figure 2, on a frontage road to the west of I-35, 20 miles south of Duluth, MN.

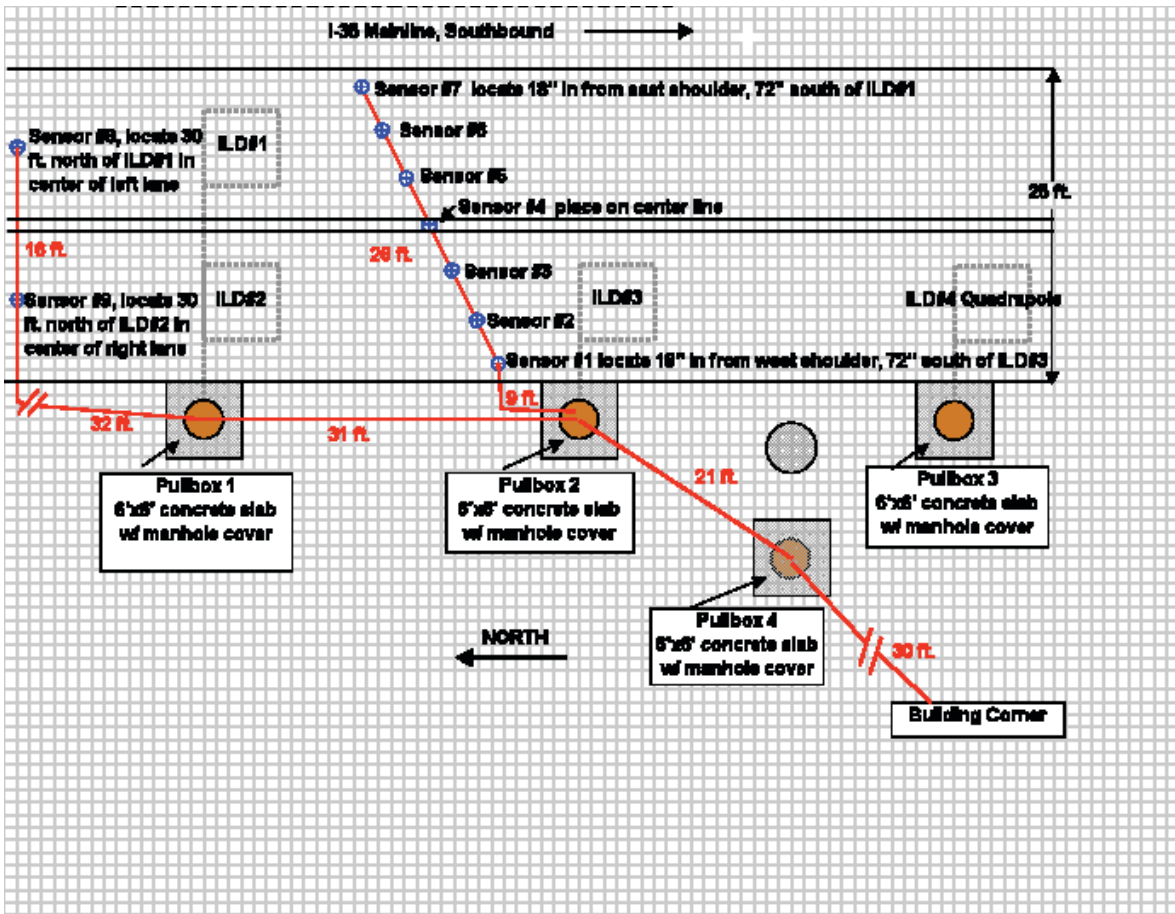


Figure 1 Magnetoresistive Array and ILD Sensor System

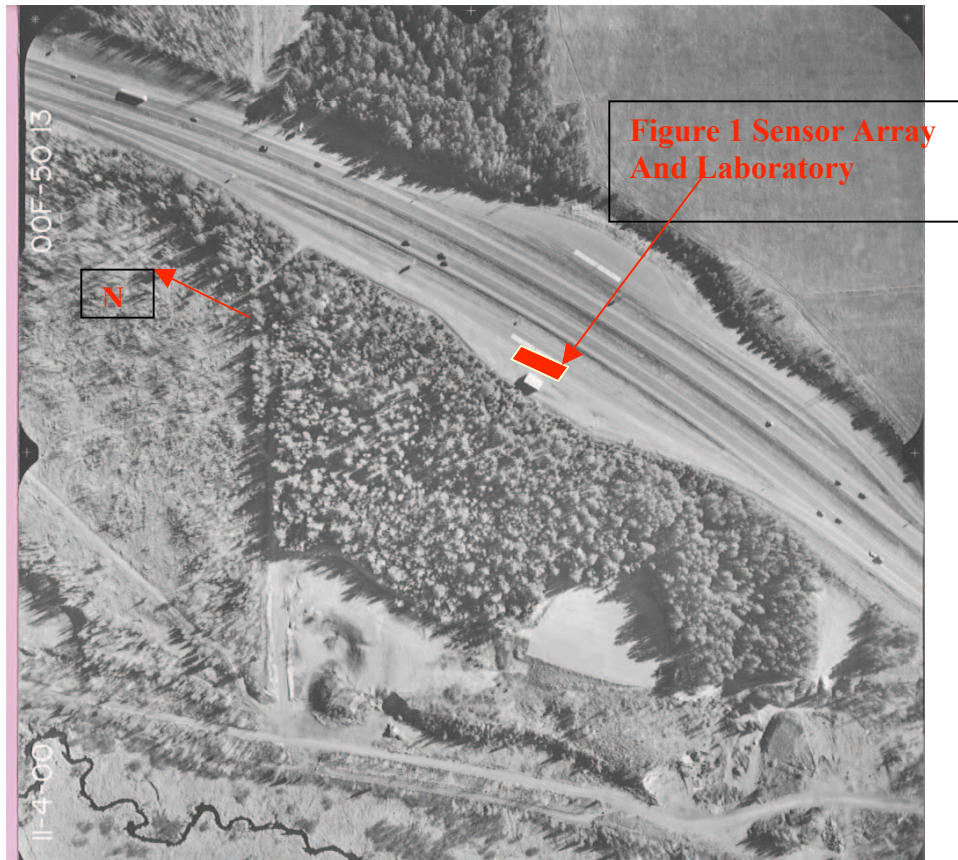


Figure 2 I-35 Test Site Marker 236 Southbound
Aerial Photograph Provided by Mn/DOT

The ILD, as a primary sensor system for traffic management has been use for decades.[1] The fundamental theory and equivalent circuits dates from the 1920's study of the behavior of flat pancake inductors used in early radio systems [2]. Much of the practical implementation and theoretical magnetostatics theory and background is summarized in Federal Highway Administration documents. [3]

Three standard 4-turn ILDs and one quadrapole are located as shown. An array of seven magneto-resistive sensors are positioned across both lanes of the frontage road. Two additional magneto-resistive sensors are positioned to serve as triggers. The spacing is designed for simultaneous collection of both ILD and magneto-resistive data including lateral and longitudinal inductance and magnetic field measurements.

ILD Time Domain Inductance Model

The measured inductance of an ILD decreases when a vehicle is within the active region of influence. [4]. This decrease in inductance is the result of induced currents, i.e. eddy currents, which significantly overcomes any net inductance increase from the increase in the relative permeability, m_r , of ferrous vehicle components such as the frame and engine. The resultant mutual inductance from the induced eddy currents requires a closed electrical path such as that provided by the vehicle frame, engine, and other, not necessarily ferrous, vehicle subsystems.

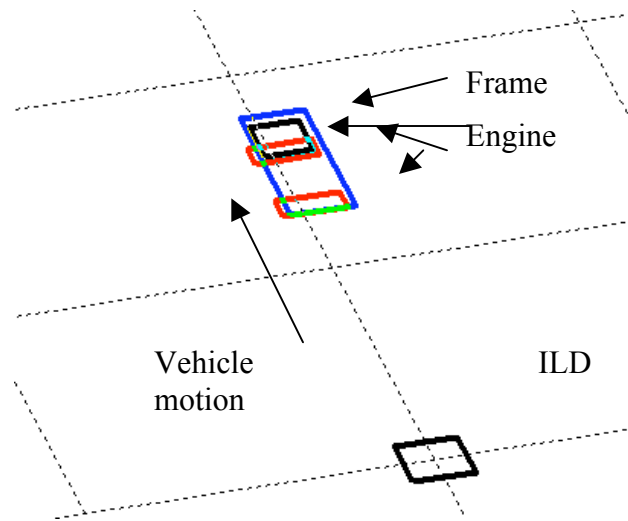


Figure 3 ILD Magnetic Field And Inductance Analysis

Figure 3 illustrates a four closed-path mutual inductance simulation model. The results of the simulation which will output a net negative inductance change of the ILD. Assuming the ILD has negligible resistance and the length of one side of loop \gg radius of wire, Biot-Savart's Law, as given below, is used to compute the magnetic field, B , and the magnetic flux density, Ψ , which is then used to obtain the ILD inductance, L , which then includes all of the mutual inductances M . Observe that there are mutual inductance interactions between all of the closed paths. Only four closed paths are used because of computational complexity. In reality, the vehicular structure is considerable more complex. MATLABTM was used for calculating the three dimensional ILD magnetic field and the resultant eddy current induced interaction with vehicles passing over the ILD. Eqn. (1) yields the ILD inductance.

$$L = \frac{N\Psi}{I} \quad (1)$$

and the flux density

$$\Psi_{21} = \int_{S_2} \beta_1 \cdot \hat{n} dS \quad \text{also} \quad \Psi_{12} = \int_{S_1} \beta_2 \cdot \hat{n} dS \quad (2)$$

must be computed for each closed path with the result for mutual inductance given by

$$M_{21} = \frac{N_2 \Psi_{21}}{I_1} \quad \text{and} \quad M_{12} = \frac{N_1 \Psi_{12}}{I_2} \quad (3)$$

Figure 4 illustrates the magnetic field intensity from a standard 1.83 m x 1.83 m ILD. The inductance is proportional the square of the number of loops in the ILD. The fringing magnetic field suggests that there may be adjacent lane phantom vehicle detection errors. Figure 5, illustrates this detection potential for both the standard ILD and to a lesser extent, for the quadrapole.

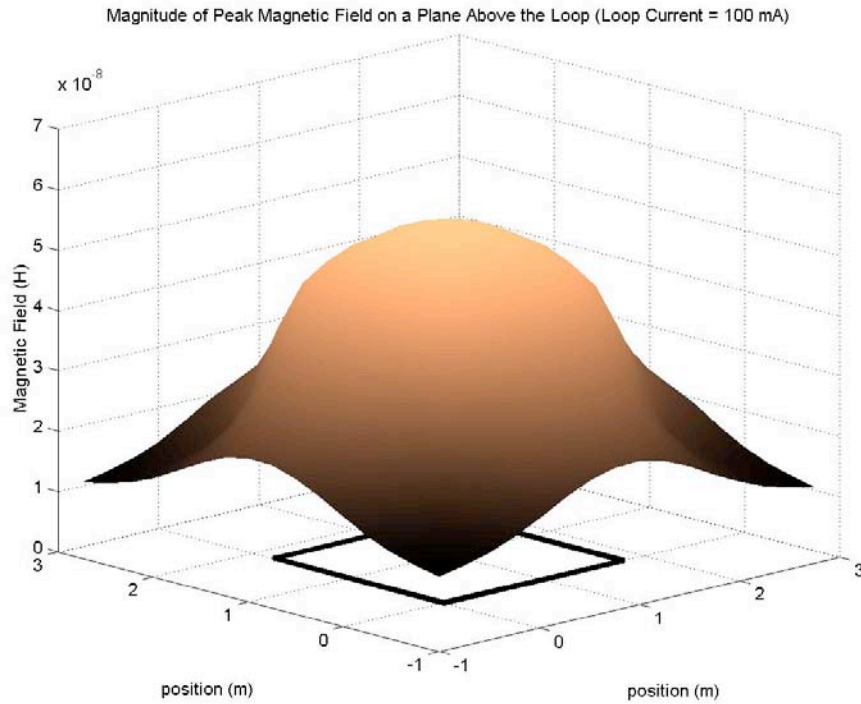


Figure 4 ILD Two-Dimensional Plot of Inductance

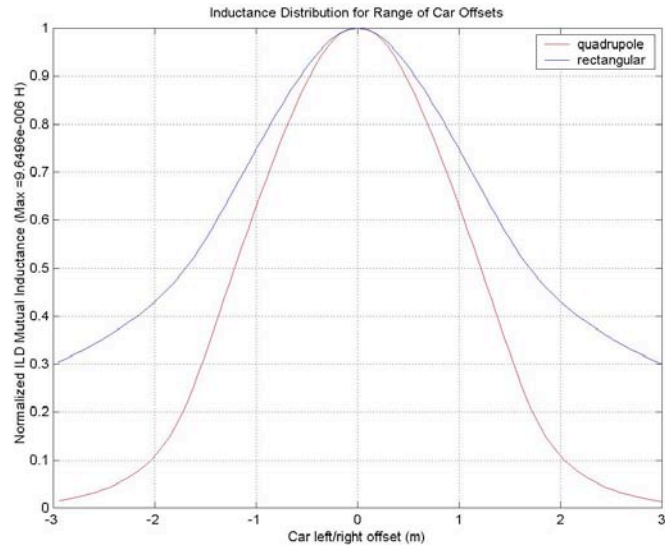


Figure 5 Cross-Section Inductance For An ILD And A Quadrapole

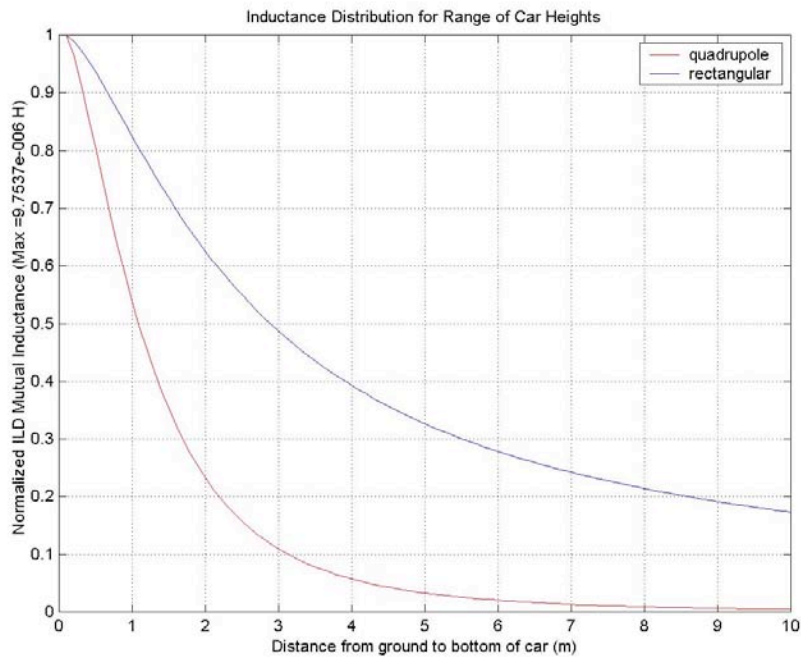


Figure 6 ILD And Quadrapole Inductance As A Function Of Height Above The Road Surface. (Center Of The Loop)

Figure 7 is an example of an ILD inductance signature obtained from a truck-trailer, “18 wheeler”. This time-domain signature is obtained by measuring the inductance every 30 ms using a LASER-triggered Agilent LCR Bridge. The inductance change from the engine/cab and axles are clearly visible. However to be more quantitative, several signal processing algorithms within MATLAB™ including first derivative signatures, n-order polynomial fits, and Fast Fourier Transforms (FFTs) have been employed to ascertain vehicle types. The measured signatures are also compared with two-four closed-path mutual inductance theoretical calculations using Eqns. 1-3. Closed path geometries were derived from an estimate of the vehicle frame, engine block, and axle dimensions. Preliminary studies on a limited number of vehicle types show that there are reasonably unique ranges of amplitude coefficients and response curves associated with different vehicles but the current 30 ms sample time measurement system does not provide adequate high vehicle speed resolution.

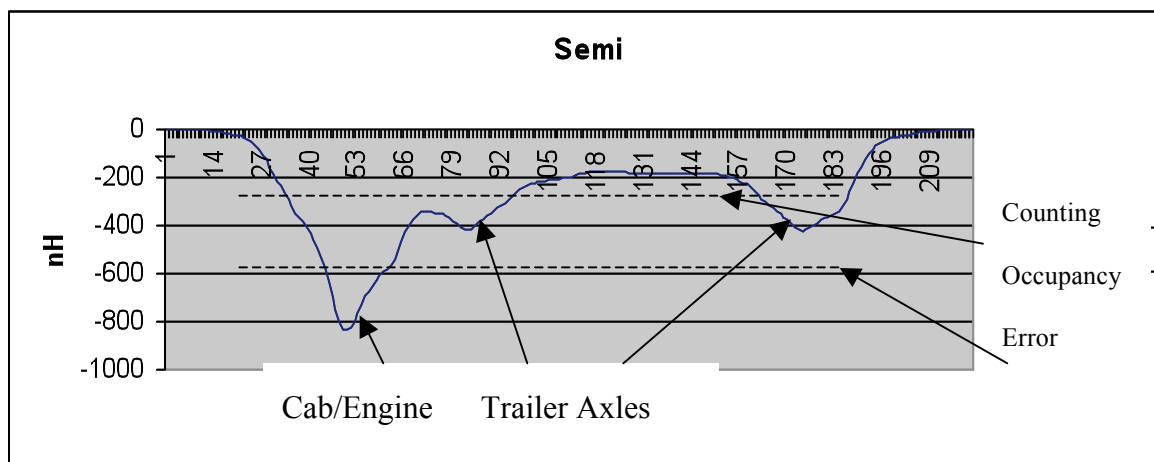


Figure 7 ILD Inductance Signature For An “18-Wheeler”.

Two different threshold settings are shown. The “Correct Count” threshold identifies occupancy for one vehicle of unknown type. The lower “Counting Occupancy Error” threshold indicates two vehicles. The velocity is under 10 mph. At higher speeds, the inductance profile becomes less defined.

Magneto-resistive Sensor Analysis

Magneto-resistance is the property of some materials to lose or gain [electrical](#) resistance under the influence of an external [magnetic field](#). A modest 5% resistance reduction was first observed by William Thompson in 1857. Contemporary devices exploit the quantum mechanical effects observed in thin film structures fabricated from very thin alternating layers of ferromagnetic and non-magnetic materials. This Giant Magneto-resistive Effect (GMR) is exploited in computer magnetic hard drives. [5]

The magneto-resistive array being used for test site vehicle signature measurements is manufactured by Banner Engineering. Each of the seven sensors is an active module which includes signal processing to reference the Earth’s magnetic field and on-board non-volatile memory. [6] Each of the sensor packages includes three orthogonal

magnetoresistive transducers and associated signal processing hardware. A serial data stream yields a 14-bit A/D digitized output voltage where a vector sum is computed using Eqn. 4.

$$V_{out} \propto (B_x - B_{ambient\ in\ x})a_x + (B_y - B_{ambient\ in\ y})a_y + (B_z - B_{ambient\ in\ z})a_z \quad (4)$$

The magnitude of the Earth's magnetic field (vector sum of $B_{ambient}$ in x, y, and z at mid-latitudes is about 0.5 G and is perturbed by nearby ferrous objects. Software is used to remove this quasi-static local magnetic field. Software is also used to remove temperature sensitivity. A key difference between the magnetoresistive sensor and the ILD is that the magnetoresistive sensor does not respond to non-ferrous metals, i.e. Al. Non-ferrous materials have a relative permeability of $\mu_r = 1$ while ferrous materials have $\mu_r \gg 1$ (usually 10s to several hundred). Consequently, the each of the magnetic field vector components is significantly and proportionally changed. This change, Eqn. 5, is what is measured and used to obtain signatures.

Figures 8, 9, and 10 illustrate the data available from the magnetoresistive array. All data is available in real-time. Figure 8 shows a single sensor magnetic field deviation from the background response in x, y, and z orthogonal axes as well as the net absolute value. The data intervals are 6 ms. The absolute counts in all seven sensors in the diagonal array to generate a signature as shown in Figure 9. When an EXCEL interpolation is applied, we have the solid profile shown in Figure 10.

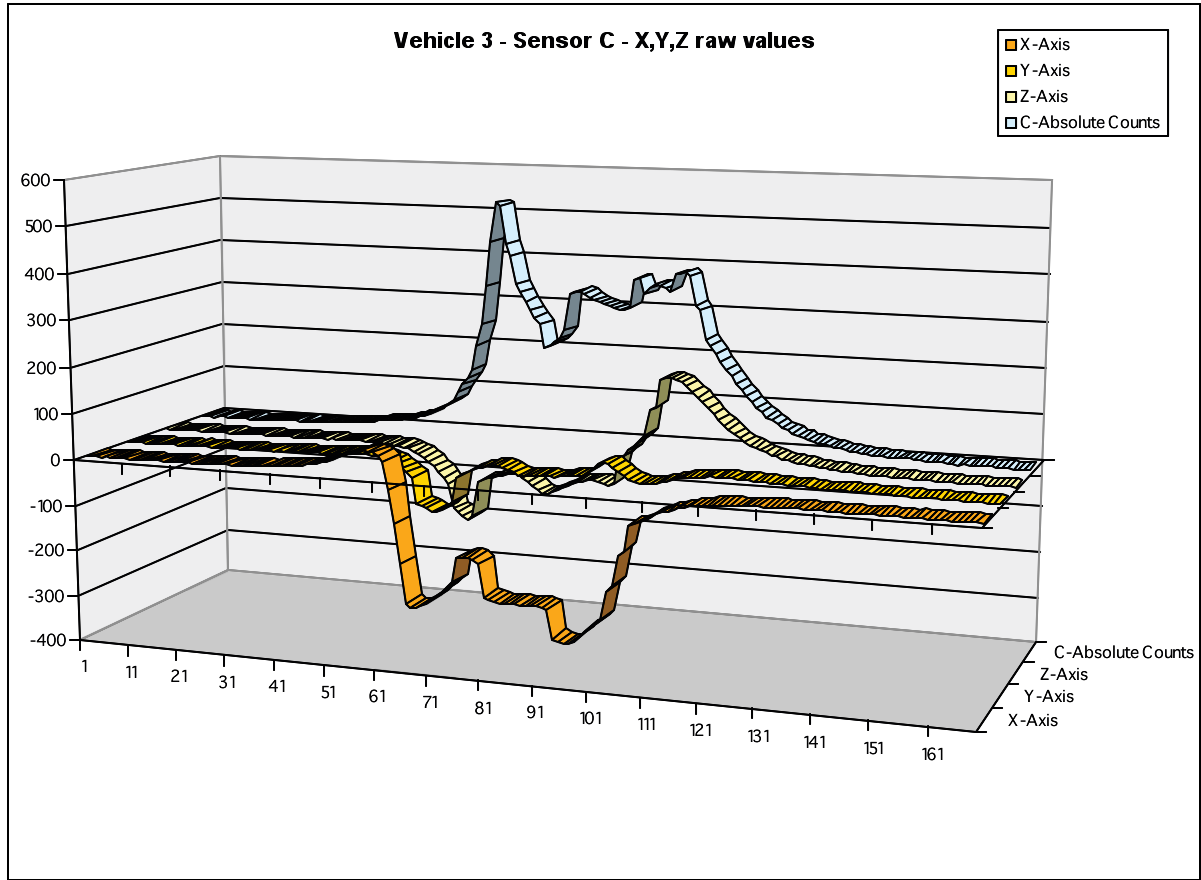


Figure 8 Single Centered Magneto-resistive Orthogonal Axes Magnetic Field Deviations and Absolute Value (The vehicle under test was 3/4 ton Ford extended cab pickup truck with a snowplow mounting frame (without plow) and winch moving at 40 mph. One can easily observe the large ferrous-induced peak from the snowplow frame structure as well as the two smaller peaks from axles.)

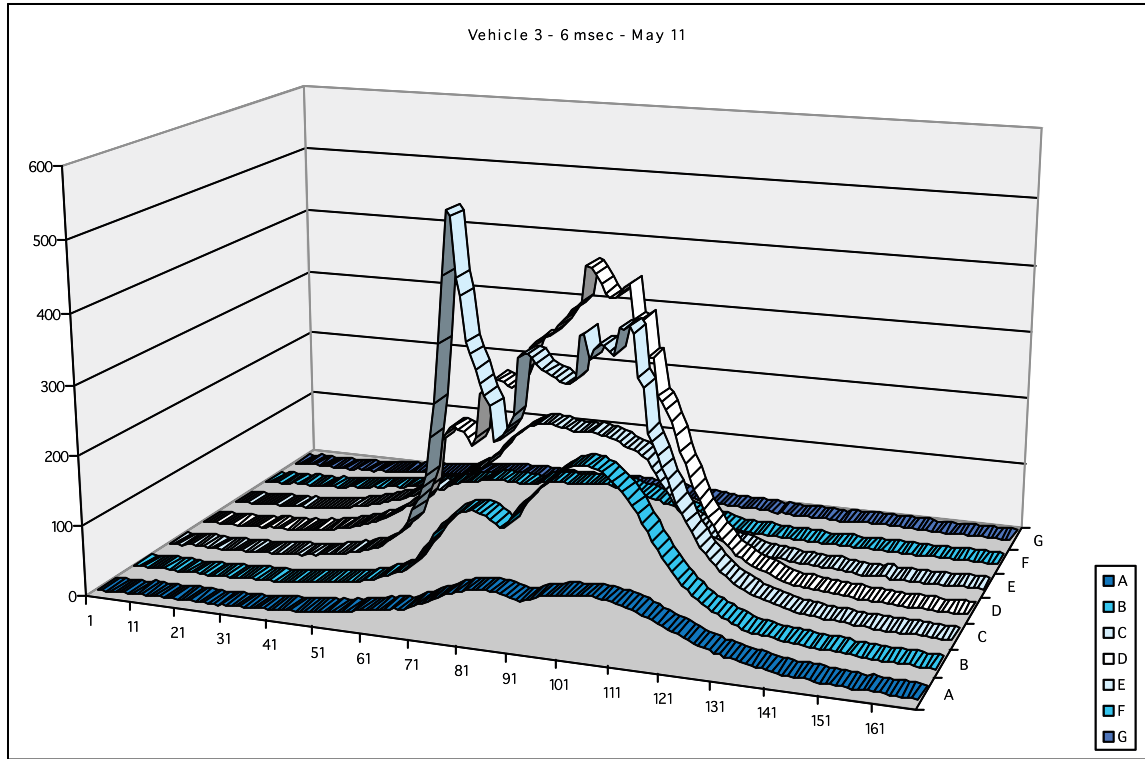


Figure 9 Seven Magnetoresistive Sensor Array Response For a ¾ Ton Pickup With Snowplow Frame

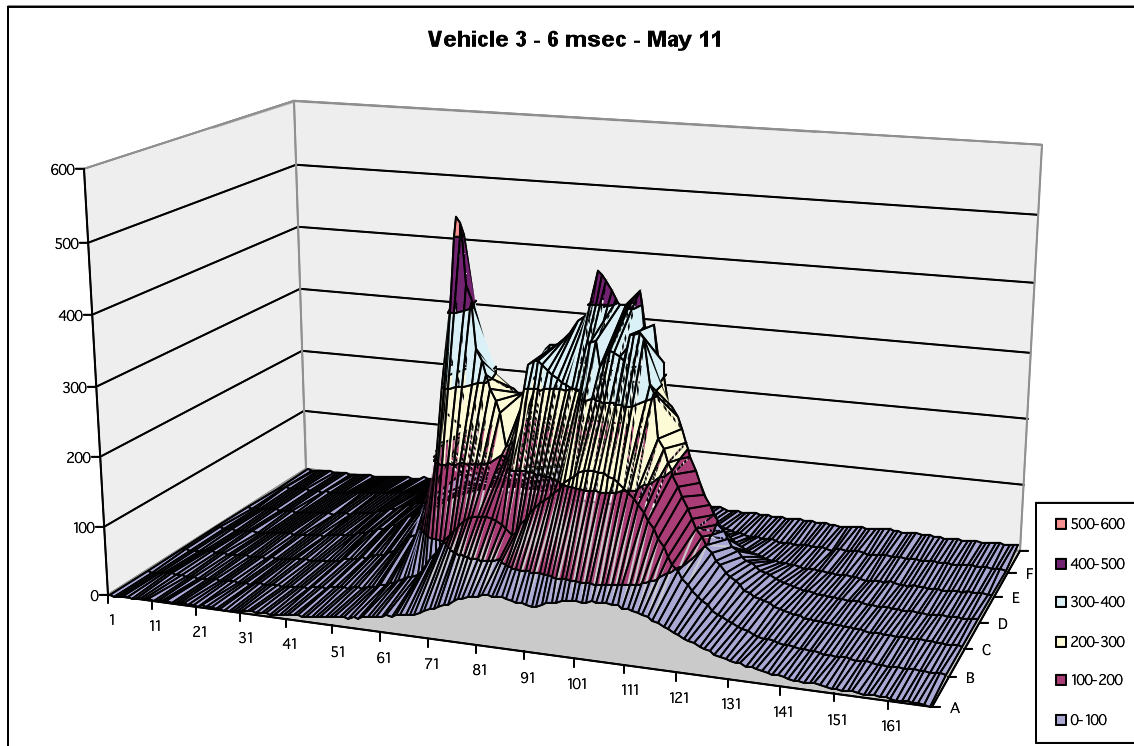


Figure 10 EXCELL Graphical Interpolation of the data In Figure 9

Summary and Directions Of Future Work

Both the ILD and magnetoresistive sensor systems have strengths and weaknesses when applied to vehicle classification and occupancy determination.

The ILD is, by far, the most widely installed sensor for traffic management. The ILD is a passive system which is generally reliable except for the stresses and strains that result in broken wires, etc. The threshold settings of the back-end electronics must be set such that smaller vehicles are not missed but if set too sensitive will falsely respond to adjacent lane vehicles and also to multi-axle vehicles. Results in reported in this paper show that these threshold type errors can be minimized by various signal processing and recognition techniques applied to the measured, non-threshold, inductance profiles. However, the large sampling area of the ILD couple with typical vehicle speeds reduces vehicular feature recognition accuracy. That is the primary reason single loop ILDs do not offer reasonable speed measurement accuracy. [7-9]

The magnetoresistive sensor is an active sensor which is also buried in the road surface but only requiring a single slit. Testing and deployment is limited. The long term reliability of an active buried sensor has not been established. It too is typically set up as a threshold sensor system for traffic management applications. However, results reported in this paper show that the effective “point source” impulse response provides far higher vehicle feature resolution at highway speeds. Signal processing and recognition software of the magnetic field perturbation signatures provide an opportunity automated vehicle type identification. If two magnetoresistive sensors were located in the same diagonal slit at a know spacing and since the this inherently high resolution system could recognize the same vehicular structural feature, speed could be obtained directly. Backup video cameras, of course not usable at night, would not be required.

To facilitate data collection and analysis, MATLAB™ based GUIs (graphical user interfaces) have been developed for both the ILD and magnetoresistive sensor array as illustrated in Figure 11. This includes overlays for best fit polynomials that are used for the classification process.

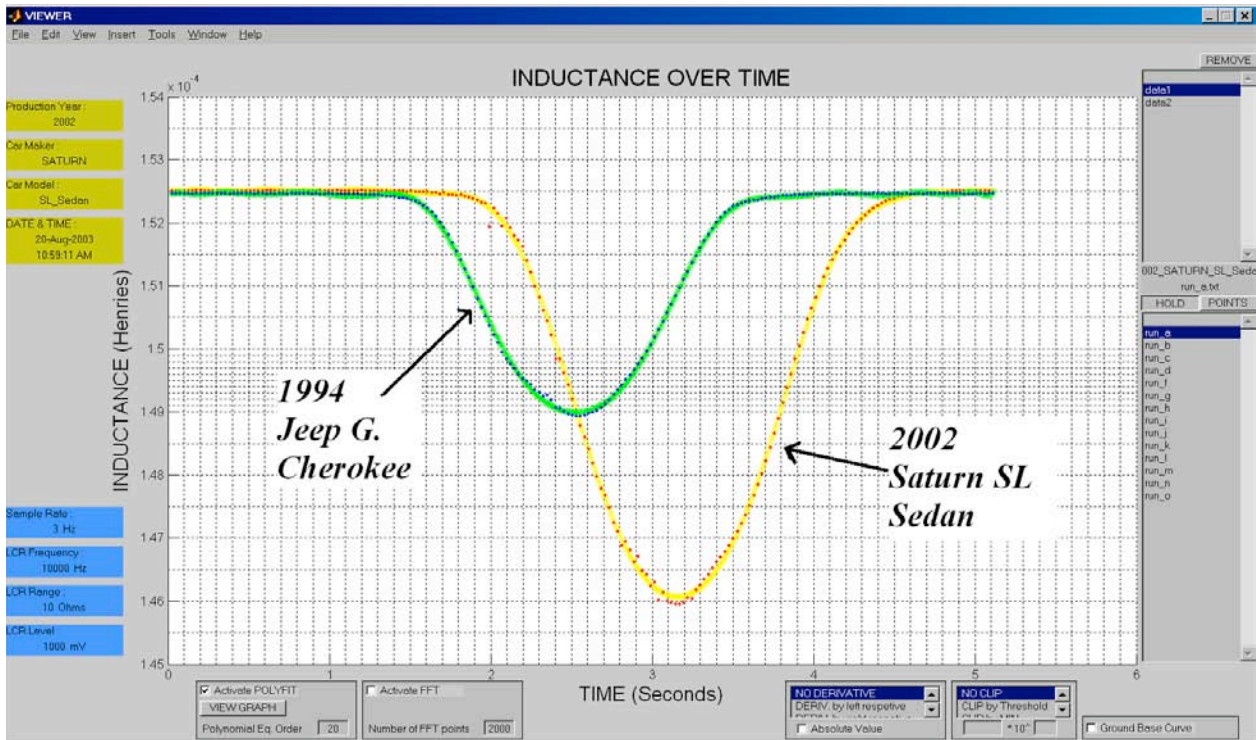


Figure 11 Sample GUI Screen

Future work will focus on:

- Preparing a three-dimensional model for different types of vehicles by mapping μ_r and use this model to predict the resultant local magnetic field distortion of a background ambient magnetic field. That is predict the resultant magnetic field distortion and resultant for a system of “chunks of iron” traveling across the sensor array.
- Comparing the model with field measurements of as many types of vehicles where classifications are delineated by the NHTSA.
- Comparing the magneto-resistive sensor signatures with the ILD signatures with respect to utility for vehicle classification, speed, and the specification of threshold setting criteria.
- Using the signatures for modeling and measurements of adjacent lane errors.

Acknowledgements

Funding was provided by the Northland Advanced Transportation Systems Research Laboratories (NATSRL), Center For Transportation Studies, University of Minnesota and the University of Minnesota Duluth. (CTS/UMD). Banner Engineering provided the magneto-resistive sensor array and associated software.

Co-Author, Timothy E. Delf, graduated with a B.S.E.C.E. degree from the University of Minnesota Duluth (UMD), May 2005. Over the last two years, electrical and computer engineering students Vikhram Gowreesunker, Jerod J. Wendt, James R. Riehl, Zachery T. Serre, and David J. Keranen, NATSRL engineer assisted in the data collection and modeling.

REFERENCES

1. *Inductive Loop Detectors*, ITS Decision Report, http://www.networking.eecs.berkeley.edu/...M/Incident_Manage/Detection/loopdet.html 1997 and 2001 updates. This site has extensive links to case studies, national and international, and assessments.
2. M. K. Mills, "Inductive Loop System Equivalent Circuit Model" *Vehicular Technology Conference of IEEE*, vol. 2, pp. 689-700, 1999.
3. *Traffic Detector Handbook, Second Edition*, Federal Highway Administration, Publication Number FHWA-IP-90-002, July 1990.
4. Carlos Sun, Intelligent Surveillance Using Inductive Vehicle Signatures, PATH, Rowan University, *Intellimotion*, Vol. 8, No. 3, 1999.
5. <http://www.research.ibm.com/research/gmr.html>
6. <http://www.baneng.com> Banner Engineering Corp. sensor technical data and http://www.bannerengineering.com/whats_new/release.php?id=71
7. Benjamin Coifman and Zu-Hsu Lee, *Estimating Median Velocity Instead of Mean Velocity at Single Loop Detectors*, Transportation Research-B, 7/11/2000.
8. Benjamin Coifman and Zu-Hsu Lee, *New Aggregation Strategies to Improve Velocity Estimation From Single Loop Detectors*, California PATH Working Paper, UCB-ITS-PWP-2000-12. August 2000.
9. Carlos Sun and Stephen G. Ritchie, *Individual Vehicle Speed Estimation Using Single Loop Inductive Waveforms*, California PATH Working Paper, UCB-ITS-PWP-99-14. October 1999.

10. Appendix E

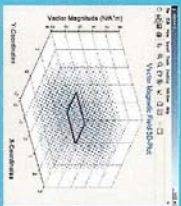
Poster #2, “Inductive Loop Detector Vehicle Signature Analysis Using Magnetic Field models, Simulations, and Measurements”

Prepared by

Stanley G. Burns, Timothy Delf (undergraduate ECE student), and Dave Keranen (staff engineer assigned to NATSRL).

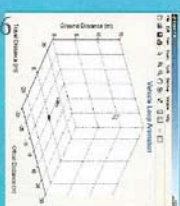
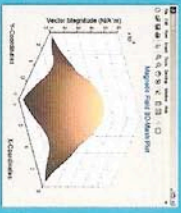
Inductive Loop Detector Vehicle Signature Analysis Using Vehicle Magnetic Field Models, Simulations and Measurements

Dr. Stanley G. Burns Timothy DeRUMD ECE Undergrad Dave Keranen

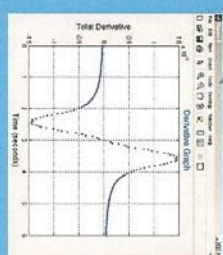
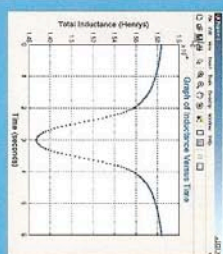


Vector Magnetic Field 3-D Plot
 Biot-Savart's Law in conjunction with superposition determine the magnetic field for the inductive loop detector. The ILD is modeled as a rectangular loop at the origin. Vectors show an increasing magnetic field closer to the ILD.

Mesh Magnetic Field 3-D Plot
 This illustration exhibits a mesh modeling of the same magnetic field above. This model clearly shows a maximum magnetic directly over the ILD, and a weaker magnetic field further from the origin. This model makes use of the Biot-Savart Law along with superposition.



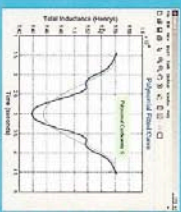
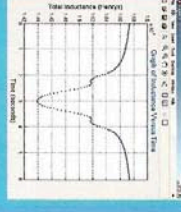
Vehicle Loop Animation
 The ILD model produces an animation sequence which is dependent upon user input. Speed, vehicle offset, and type of modeling desired are all factors taken into consideration for the animation. The ILD is modeled as the rectangular loop at the origin.



The objective of the Inductive Loop Detector research is to model and measure the vehicle-induced time domain inductance profile to identify the vehicle class by using various signal processing techniques. The magnetic field models work in conjunction with the ILD simulation to determine the change in flux through a vehicle modeled as many rectangular loops. The changing flux can then be used to find the mutual inductance between the different components of the vehicle. The total inductance is then calculated with respect to time and then plotted. The user provides dimensions of the vehicle, along with speed and offset. The graphs above show simulations of a 1999 Ford Taurus SE. The first graph being the inductance signature and the second being its derivative.

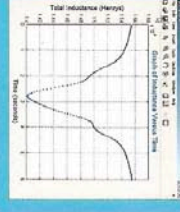
Previous work sampled real-time data from different vehicle. This system was connected to a laser trigger, and when broken, would collect 200 data points corresponding to the inductance and time. The program would then graph the ILD signature and provide manipulation techniques to examine the results. Pictured below is the graphical user-interface of the system.

Vehicle Simulation Body and Axes
 This simulation included only the body and axes of the vehicle, which were modeled as rectangular loops. The decreased areas of inductance on both sides of the signature indicate times of high iron concentration. This indicates the axes crossed over the ILD at these two times.



Vehicle Identification
 Identification through the ILD signature using polynomials to determine the best fitting coefficients. Depending upon the number of coefficients entered, the model will approximate a curve to actual signature and display the resulting coefficients.

Body, Axes and Engine Plot
 The graph to the right shows the result of all components being modeled simultaneously. The final result shows areas indicating the axes along with a forward shift in the plot due to the included engine loop. The outcome is similar to real-world data collected.



Appendix F:
Poster #1, “Inductive Loop Detector Signal Analysis”

Prepared by

Stanley G. Burns and Jerod Wendt (undergraduate ECE student).

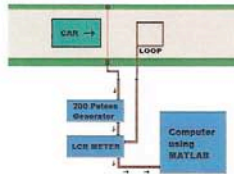
Poster outlines the custom software signal processing algorithms used to process ILD data with a dedicated differential inductance measuring system.

Inductive Loop Detector Signal Analysis

Dr. Stanley G. Burns Jerod Wendt (UMD ECE Undergrad)

The objective of the Inductive Loop Detector research is to model and measure the vehicle-induced time-domain inductance profile to identify the vehicle class by using various signal processing techniques.

Sampler Program

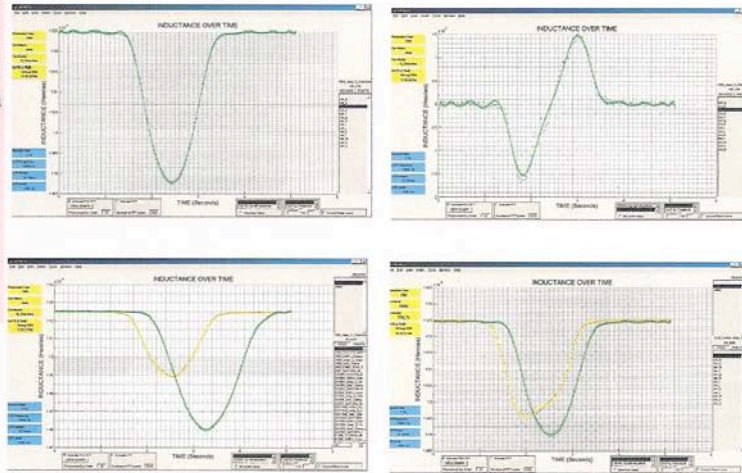
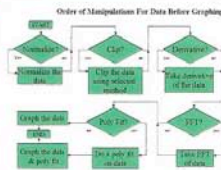


The Sampler program controls the equipment in the list below to gather data and to save it in a text file. The system will sample data and save it anytime that the laser beam is broken.

- 1) Agilent 4263B LCR Meter
- 2) Agilent 33120A Function Waveform Generator
- 3) Agilent E3631A Triple Output Power Supply
- 4) National Instruments DAQ card
- 5) BANNER Q45BB6LLQ Laser Diode Retroreflective Sensor

Viewer Program

The VIEWER program is used to view and manipulate the data that is produced by the Sampler program. The provided data set manipulations are Normalize, Clip, Derivative, FFT, and the Polyfit. The data manipulation procedure follows the order shown in the flow diagram below.



Identifier Program

The Identifier program is used to try and identify a unknown profile with a known one. The Identification is based on the average of five curves from each vehicle in data base. Averages are based on polyfit coefficients and procedure of identification is described in the charts to the right.

Method of Identifying

	X ⁻³	X ⁻²	X ⁻¹	X ⁰	max. value
UDO	0.0000	0.0000	0.0000	0.0000	0.0000
Vehicle #1	0.0000	0.0000	0.0000	0.0000	0.0000
Vehicle #2	0.0000	0.0000	0.0000	0.0000	0.0000
Vehicle #3	0.0000	0.0000	0.0000	0.0000	0.0000

The UDO is identified as the vehicle with the largest $\sum_{i=1}^n C_i$ value.

How Point Amount is Determined

	Vehicle #1	Vehicle #2	Vehicle #3	Amount of points the coefficient is worth.
X ⁻³	STD	STD	STD	(SUM) = *
MEAN	(STD/Max)	(STD/Max)	(STD/Max)	(SUM) = *
X ⁻²	STD	STD	STD	(SUM) = *
MEAN	(STD/Max)	(STD/Max)	(STD/Max)	(SUM) = *
X ⁻¹	STD	STD	STD	(SUM) = *
MEAN	(STD/Max)	(STD/Max)	(STD/Max)	(SUM) = *
X ⁰	STD	STD	STD	(SUM) = *
MEAN	(STD/Max)	(STD/Max)	(STD/Max)	(SUM) = *

The above two charts are a rough example using a poly fit of three coefficients.